DEVELOPMENT OF IMMUNOASSAY USING GRAPHENE AND MICROFLUIDIC PLATFORMS

by

Huai-Ning Chang

A dissertation submitted in partial fulfillment
of the requirements for the degree of
Doctor of Philosophy
(Biomedical Engineering)
in The University of Michigan
2015

Doctoral Committee:

Professor James R. Baker Jr., Co-chair
Professor Theodore B. Norris, Co-chair
Professor Mary-Ann Mycek
Professor Suichi Takayama
Associate Professor Zhaohui Zhong

To my family

ACKNOWLEDGEMENTS

First and foremost, I would like to thank my research advisors who supported me throughout the doctoral training:

Dr. James Baker, for supporting me with great resources and good environments to conduct my research. Without his support, this degree would not have been possible. I am deeply indebted for that as well as for the training received with which I have truly broadened my perspective.

Dr. Ted Norris, for his mentorship and guidance. I am benefited from his enthusiasm in research and optimism when facing dilemma. Finally, I truly appreciate his trust in letting me take on high level responsibilities.

I would like to express my appreciation to the members of my dissertation committee; their broad knowledge always reminds me to continue learning for a lifetime.

Dr. Mary-Ann Mycek, for her contributions as a thesis committee member. Her work attitude and morale boost to students are highly valued.

Dr. Shuichi Takayama, for his contributions as a thesis committee member and his enthusiasm for excellence in research.

Dr. Zhaohui Zhong, for being extremely generous with sharing his knowledge, lab equipment, and experimental materials. I am grateful to him and his group for the help with graphene production and handling.

I have received tremendous and diverse support and training from experiments and scientific discussions and want to thank the following individuals for sharing their knowledge with me.

Present and past members of The Michigan Nanotechnology Institute for Medicine and Biological Sciences (MNIMBS):

Dr. Sascha Goonewardena, for his dedication in training his team to learn to write in the discipline, and for his assistance with the microfluidic projects.

Dr. Pascale Leroueil, for her assistance with the microfluidic projects. I also appreciated her experience sharing and the discussion.

Dr. Hong Zong, for providing fundamental teaching in organic chemistry and macromolecule synthesis.

I am very grateful to the previous and current staff of MNIMBS, Claire Verweij, Pat Bergeron, and Mike Parise, for their administrative support and kindness.

I have a deep connection with the people that I worked with, and with whom I share the memory of my PhD life. Thanks to my colleagues who provided me scientific and moral support, and were always ready to lend a helping hand. From Dr. Norris's group, I would like to especially thank Heather, Miao-Bin, and You-Chia, for not only the support in experiments, but also for getting me involved in the group when I first joined. In Dr. Baker's group, the following people are specially thanked: Shengzhuang Tang and Dr. Ming-Hsin Li for creating a vibrant work environment.

Lastly, I would like to acknowledge the financial support provided from the BME Department and Chia-Lun Lo Fellowships from Rackham Graduate School.

My utmost appreciation goes to my family and friends. I deeply appreciated my tea time friends in Ann Arbor and I could not have made it this far without their support and faith.

TABLE OF CONTENTS

DEDICATION ……..……ii

ACKNOWLEDGEMENTS……..…….……..….iii

LIST OF FIGURES…….....……..viii

ABSTRACT…….……...x

CHAPTER 1 .....……..…….....1

PROTEIN IMMUNOASSAY AND ITS DEVELOPMENT

1.1 Introduction…….……..……1

1.2 Overview of protein immunoassay…….……..…….1

1.2.1 Protein immunoassay forms – The principles of how it works…….…….....2

1.2.2 Competitive immunoassays…….…….....3

1.2.3 Non-competitive immunoassays……..…….....3

1.3 Protein immunoassay development goals……..…….....4

1.3.1 Specificity…….....4

1.3.2 Efficiency…….....5

1.3.3 Sensitivity.....7

1.4 Immunoassay platform.....8

1.5 Other goals.....9

1.6 Graphene in biosensing.....9

1.7 Dissertation map.....10

1.8 References.....11

CHAPTER 2 ...…….15

FLUOROPHORE AND PROTEIN CONJUGATED DIELS-ALDER FUNCTIONALIZED CVD GRAPHENE LAYERS

2.1 Introduction……..……15
2.2 Materials and Methods……..……...17
2.3 Results and Discussion…….……...20
2.4 Conclusions……..….....25
2.5 References…….....30

CHAPTER 3...…….....33

PROFILING INFLAMMATORY RESPONSES WITH MICROFLUIDIC IMMUNOBLOTTING

3.1 Introduction.....33
3.2 Materials and Methods.....34
3.3 Results and Discussion.....36
3.4 Conclusions.....41
3.5 References.....46

CHAPTER 4 48

DOT BLOTTING USING MICROFLUIDIC TECHNIQUES

4.1 Introduction……..……48
4.2 Materials and Methods……..……...49
4.3 Results and Discussion…….……...53
4.4 Discussion……..……..59
4.5 References……..……..61

CHAPTER 5 ……...…….63

CONCLUSIONS

5.1 Summary……..……63
5.2 Summary of functionalization of graphene……..……63
5.2.1 Functionalization of graphene: covalent approaches……..……...64
5.3 Future steps of developing graphene biosensing platform…….…….65
5.4 Summary of applying microfluidic techniques to immunoblotting……..…...66
5.5 Summary of cytokine detection using microfluidic dot blotting……..…67
5.6 Summary of cytokine detection using microfluidic dot blotting……..…68
5.7 Future steps for applying microfluidic techniques to immunoblotting and dot blotting…….....69
5.7.1 Surface Modification and Immobilization…….……..……..69
5.8 Prospects…….…70
5.9 References……..…..71

LIST OF FIGURES

CHAPTER 1

Figure 1.1: Schematic diagram of the competitive binding assay……...…3

Figure 1.2: Schematic diagram of the non-competitive binding assay……...….4

Figure 1.3: Two principles of multiplex assays……...……6

CHAPTER 2

Figure 2.1: Raman spectroscopy of graphene……21

Figure 2.2: Fluorescence images of Alexa 488 cadaverine conjugated graphene…….22

Figure 2.3: The XPS spectra of pristine CVD graphene and DA-functionalized graphene conjugated with Alexa 488 cadaverine……..24

Figure 2.4: Fluorescence images of BSA conjugated graphene……25

Figure 2.5: Alexa 488 cadaverine conjugated to Diels-Alder reaction functionalized graphene visualized under fluorescence microscopy…….27

Figure 2.6: MALDI-TOF mass spectroscopy characterization of BSA proteins conjugated with Alexa 488 carboxylic acid, succinimidyl ester……..28

Figure 2.7: PMMA layer and pristine graphene visualized under optical microscopy and fluorescence microscopy……29

CHAPTER 3

Figure 3.1: Schematic of a PDMS microfluidic device and the interface with a PVDF membrane……...37

Figure 3.2: Comparison of traditional and microfluidic immunoblotting in human blood monocyte samples……..38

Figure 3.3: Detection of STAT3 phosphorylation in response to inflammatory stimuli...41
Figure 3.4: Protein immunoblots of the MAPK pathway using different chemiluminescent detection modalities…….43

Figure 3.5: Comparison of antibody and protein signal dependence of traditional and microfluidic protein immunoblotting…….44

Figure 3.6: Example of microfluidic protein immunoblot generated using a 5-channel per lane microfluidic device…….45

CHAPTER 4

Figure 4.1: Schematic of microfluidic dot blot system……..50

Figure 4.2: Comparison of traditional and microfluidic dot blotting in macrophage supernatants……54

Figure 4.3: Protein lane width variation at different protein concentrations…….56

Figure 4.4: Protein lane width variation at different PVDF membrane surface wetting properties……57

Figure 4.5: Detection of inflammatory cytokines in response to inflammatory stimuli…59

Figure 4.6: 2.5 mg/ml protein lane width measurement by intensity profile line scan…..60

ABSTRACT

Protein, as one of the most important functional biomolecules in the human body, plays a significant role in physiological responses and molecular diagnostics. Detecting the existence of proteins, quantifying concentration, and identifying protein types are therefore important techniques in many fields. There is also a need to develop protein detection techniques that provide high efficiency, low cost, and high sensitivity. Immunoassays are one of the major techniques relied on for protein detection. Immunoassays have been broadly applied in disease diagnosis, pharmaceutical development, food science, and environmental protection. Significant impacts in these fields have motivated people to develop immunoassays with better performance in terms of efficiency, sensitivity, specificity, and point-of-care feasibility.

The first part of this dissertation describes studies aimed at developing chemical vapor deposition (CVD) graphene as a large size protein biosensing platform. Since the first success of graphene isolation in 2004, a tremendous number of potential applications of graphene have been proposed. In particular, the application of graphene to biosensor development has received a great deal of interest. To utilize graphene as a biosensing platform, techniques to immobilize proteins on graphene are critical. In this dissertation work, carboxyl functional groups (-COOH) were created by graphene functionalized through Diels-Alder reaction followed by hydrolysis, and the functionalized graphene was characterized using Raman spectroscopy, X-ray photo spectroscopy (XPS), and fluorescence microscopy. These methods help to characterize the creation of the carboxyl functional groups, the functional groups distribution uniformity and their density. The fluorescence images show that the carboxyl groups were created uniformly. The XPS results in carboxyl group density approximation of 22%. The approach developed here provides information about protein coupling density and uniformity on large scale graphene (> cm^2).

The second and the third parts of the thesis describe the application of a microfluidic technique to two widely used protein detection methods – immunoblotting and dot blotting. Applying microfluidics to protein immunoblotting and dot blotting helps to save sample volumes, and also permits the detection of multiple proteins simultaneously. The microfluidic systems were designed and fabricated to be easily interfaced with a common type of protein blotting membrane called polyvinylidene fluoride (PVDF) membrane. The microfluidic device was specifically applied to the antibody incubation step, which reduces antibody consumption and therefore also significantly reduces the cost of the assay. In microfluidic immunoblotting, an approach to activate the PVDF membrane to increase its protein binding capacity was developed. This was achieved by adding a surfactant Tween-20 to the antibody solution. The concentration of Tween-20 was optimized so that only the portion of the membrane within the channel region was activated. The system has been shown to be able to profile inflammatory signaling pathways. In microfluidic dot blotting, the influence of substrate hydrophobicity and protein concentrations on device design constraints were studied. Inflammatory cytokine detection using the developed microfluidic dot blotting system was determined. Altogether these experiments demonstrate that applying microfluidic techniques to protein immunoblotting and dot blotting improves detection efficiency, and reduces cost by utilizing less antibodies.

CHAPTER 1

PROTEIN IMMUNOASSAY AND ITS DEVELOPMENT

1.1 Introduction

The ability to detect biomolecules is of great significance in clinical diagnostics, food safety, drug screening, and environmental evaluation. Biomolecule detection with high sensitivity and specificity are often applied in testing food that contains antibiotics, toxins, and hormones; screening patient samples including blood, saliva, and urine for disease diagnosis; and identifying pollutants that impose risks to our environment.

Among all biomolecule detection methods, protein detection is among the most important, especially considering its role in disease biomarker detection. The presence and concentrations of certain proteins can be used to indicate diseases status. These proteins can therefore be identified as biomarkers and their specific occurrence can be applied in monitoring related disease. The detection of proteins plays a critical role in disease diagnosis and screening, and various techniques have been developed for protein detection. One major method of protein detection is accomplished by immunoassays through antibody-antigen binding process. Therefore, understanding how immunoassays work and advancing their development is important in disease treatment, drug development, clinical diagnostics, and biomedical science.

1.2 Overview of protein immunoassay

Due to the significance of proteomics in disease diagnosis and therapeutic applications, profiling proteins and their modification has long been of great interests in the fields of molecular biology and clinical diagnostics. Since proteins can indicate the state of disease progression and the functions of normal biological processes within the human body, they have become important biomarkers for disease diagnosis and screening. Specific proteins have been identified as

biomarkers to address a variety of diseases including cancer, cardiovascular disease, and infectious diseases (i.e. tuberculosis, HIV).

Various techniques have been developed to profile proteins, which include enzyme-based detection techniques, florescent-protein-based biosensors, surface plasmon resonance (SPR), and nanoparticles. The most common method for protein detection in basic research and clinical diagnostics is the enzyme-linked immunosorbent assay (ELISA) [1]. Mass spectrometry also plays a major role in protein analysis [2, 3]. However, because these assay methods can only be used to analyze one or few samples at a time, they are not suitable for high-throughput screening and not efficient in assay reagent consumption [4-6].

Limitations of existing proteomic technologies have consequently driven the development and investigation of novel tools for the proteomics research. An emerging technology is the protein microarray, which is developed using the concept similar to the current DNA microarray technique[7] [8-10]. In protein microarrays, arrays of capture proteins are bound and can be used to profile protein expression [11, 12]. However, protein microarrays are limited by the biochemical diversity and the sheer number of proteins, which make an equivalent analysis much more complex and difficult to accomplish.[13]

The broad impacts of protein sensing and the demand for fast and reliable medical tests to identify large number of biomarkers have driven the development of new analytical approaches that are of high efficiency, sensitivity, specificity, and stability. This development is significant for clinical analysis and medical diagnostics due to the need to provide timely or even early detection, diagnosis, and therapy.

1.2.1 Protein immunoassay forms – The principles of how it works

The principles of protein sensing rely on antibody-antigen binding interactions. With the consideration of the nature of the analyte, labeling chemistry availability, the required assay sensitivity, dynamic range, and precision, the immunoassay methods can be classified in two basic forms: (I) heterogeneous immunoassays and (II) homogeneous immunoassays. They are distinguished by the separation process. Homogeneous assays are accomplished by simply mixing the reagent samples, and heterogeneous assays are often carried out with washing and separation steps. The design of both forms can be further classified as competitive or non-

competitive immunoassays. The choices are based on the nature of the analyte, labeling chemistry availability, the required assay sensitivity, dynamic range, and precision. The following section shows the competitive and non-competitive design, using antigen or antibody immobilized on a solid surface.[14]

1.2.2 Competitive immunoassays

The principle of competitive assays relies on the labeled and unlabeled ligands' competitive binding reactions for limited antibody binding sites. In competitive assays, a fixed amount of labeled ligand and the unlabeled ligand from the samples are incubated with the antibody at the same time. If the concentration of the unlabeled ligand increases, available binding sites for the labeled ligand decrease and result in weaker signals. Therefore, the lower the signal, the more unlabeled analyte is in the sample. This results in a negative slope for the standard curve of a competitive binding assay as shown in Figure 1.1.[15]

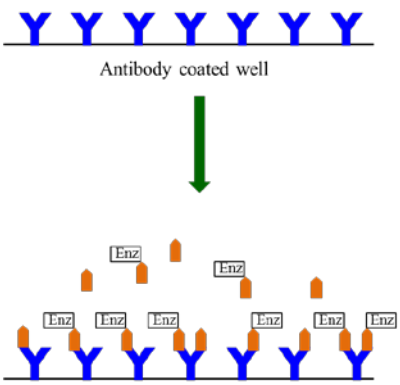

Figure 1.1 Schematic diagram of the competitive binding assay.

The antibodies are immobilized on the substrate. Both labeled and unlabeled ligands are competing for the antibody binding sites.

1.2.3 Non-competitive immunoassays

In non-competitive assays, the measurement of labeled ligand is directly in accordance with the amount of antigen present in the sample. This format of immunoassay usually provides higher sensitivity and specificity than other assays, and the standard curve of non-competitive immunoassays shows a positive slope (Figure 1.2). The most representative example of non-competitive immunoassays is sandwich ELISA.

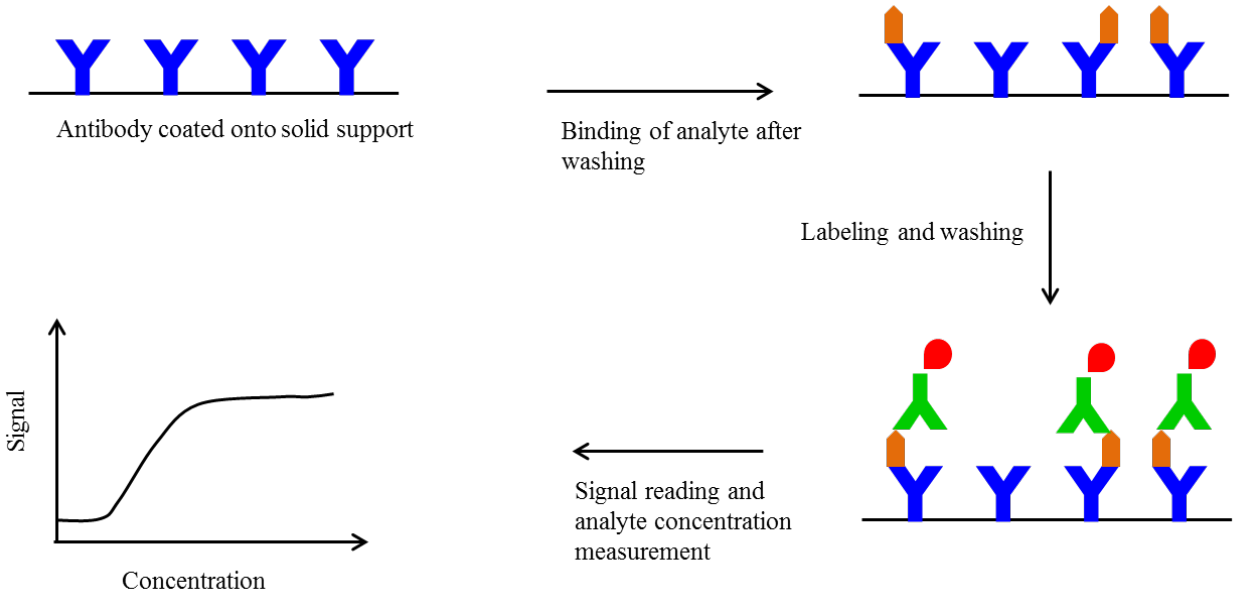

Figure 1.2 Schematic diagram of the non-competitive binding assay.

The antibodies are immobilized on the substrate. The signals are directly proportional to the sample concentration so the standard curve has a positive slope.

1.3 Protein immunoassay development goals

Immunoassays have advanced dramatically since their first introduction in 1960s. The application of immunoassay techniques in many fields such as pharmaceutical analysis and disease diagnosis usually involves measurement of great varieties of very low concentration samples. Therefore, immunoassays with good utility need to be of high specificity, through-put, and sensitivity.[14] [16] Following are some of the major goals for current immunoassay development.

1.3.1 Specificity

Specificity is a principal determinant for the quality of immunoassays since interference in assay measurements can lead to incorrect results including inaccurate concentration or analyte activity. Immunoassay specificity can be influenced by the binding property of the antibody, antigen and matrix composition, reagents, and immunoassay format. The nature of the interference may be caused by unsuspected binding proteins interfering with the reaction between analyte and assay antibodies, and antibody induced conformational changes in antigen. [17]

The specificity in immunoassays comes from the capability of the antibody to distinguish between differences in the primary structure of antigen, its optical or spatial configuration, and differences in charge [18]. It is critical to optimize antibody quality by testing potential detector antibodies against related “near neighbor” antigens to maximize specificity and determine cross-reactivity. The results can be used to select antibodies with maximum sensitivity and specificity for the target antigen [16].

1.3.2 Efficiency

As knowledge in the fields of proteomics and genetics grows, there is a growing demand for technologies that are able to extract huge amounts of information from limited sample amounts. The ability to obtain a lot of information with limited amounts of clinical samples helps to provide patients with better quality disease diagnosis, prognosis, and treatment. This demand has also driven immunoassay development to be low-cost, flexible, and high-throughput for simultaneous detection of multiple proteins in a single test. Multiplex assays are highly efficient tools designed to simultaneously measure multiple analytes in a single run/cycle of the assay. Multiplex proteomic assays for biomarker detection are of great utility in clinical settings with the benefits in screening diseases in a rapid, precise, and cost-effective way. In clinical analyses and medical diagnostics, the demand for increasing numbers of identified biomarkers and for providing fast and reliable medical tests for early detection, diagnosis, and better therapy drive the development of new analytical approaches that can be used in clinical biochemistry.

Recent advances in technology (e.g. fluidics, optics, novel material) [19-21] have facilitated a great variety of multiplex immunoassay emerging on the market. Two of the most important renovations of protein multiplex assays – the planar multiplex assay and bead-based multiplex assay – will be discussed below (Figure 1.3) [22-25].

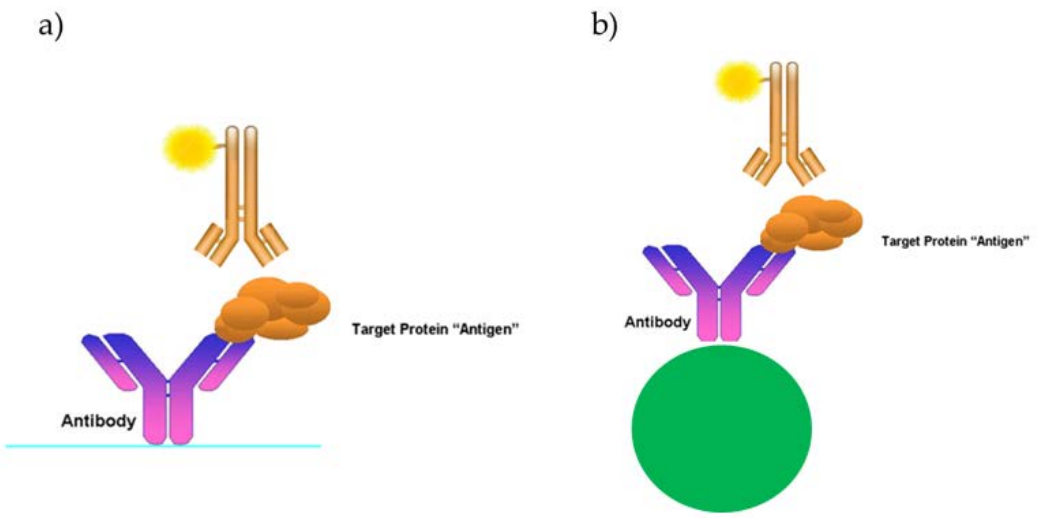

Figure 1.3 Two principles of multiplex assays.

(a) The planar microarray consists of proteins or antibody dense spots immobilized on a surface. (b) Optically encoded beads reveal antibody-antigen binding information by reading the particle code.

Multiplex planar assays

The planar multiplex assay basically consists of arrays of miniaturized and dense protein and antibody spots (typical size: ~ 300 μm in diameter; ~ 2000 spots/cm^2). This assay can be used to measure the abundance of specific proteins from the samples. Fluorescence and chemiluminescence are the most common signal detection approaches [26] [27] [28].

The planar multiplex assay platform can be nitrocellulose filters, glass slides, or hydrogel for protein immobilization. The principle of detection is like a normal ELISA, but certain limitations include: (1) it requires certain spatial separation of captured proteins on the assay platform, and (2) the detection relies on using a CCD-based imager. [29]

Encoded Bead Assays

Bead-based assays are one version of the ligand encoded microparticle array and they provide many advantages over the 2-D planar protein/antibody assays. In bead-based assays [25], beads are usually optically encoded and the optical signals are used to indicate the captured analytes in immunodetection. For example, one of the most well-known encoded bead assays is Luminex xMAP (Multi-Analyte Profiling). In Luminex xMAP, each set of beads contain a unique blend of flurophores at different concentrations which shows unique fluorescence intensity. Each set of

beads are coated with a specific type of antibody/antigen and the binding reaction changes the beads fluorescence signature. The fluorescence measurements can subsequently be used for sample concentration quantification over a wide range. This bead-based assay system has been well-established and has been successfully applied in many fields such as drug monitoring [6] [30].

The encoded bead assays are highly promising candidates for multiplex assays and the detection efficiency is achieved by preparing bead sets of different florescent dyes at various concentrations. Different sets of beads can be combined and mix with each sample. Each bead's fluorescence spectrum is recorded which provides the information of the bind biomolecules, and up to one hundred different detection reactions can be measured simultaneously [31] [4].

The major differences between encoded bead assays and multiplex planar assays are (I) encoded bead assays use fluorescence as a reporter system where multiplex planar assays use enzyme amplification of a colorimetric substrate. (II) Bead-based assays capture ligands onto spherical beads in suspension; the curved surfaces on beads provide less steric hindrance and better diffusion efficiency than the flat surface of 2-D planar assays. (III) Bead-based assays by nature achieve multiplexity by mixing multiple ligands simultaneously, which sets a more stringent condition for antibody cross-reactivity.

In summary, planar protein microarray and bead-based assays are the two major forms of multiplex protein assays. Their improved detection efficiency has significant contribution for a wide range of application includes disease early detection and therapeutic drug monitoring. However, there are still many challenges to overcome when people develop protein assays from "single-lex" to "multiplex". Therefore, there is still a need for the development of reliable, cheap, high efficiency and rapid protein sensing approaches that fulfill the demands for both basic research and clinical diagnostics.

1.3.3 Sensitivity

One major application of immunoassays is in disease diagnosis and treatment evaluation. Immunoassays are used to detect protein biomarkers, which usually circulate in blood or exist in serum. In the early stages of some diseases such as cancer, the level of the biomarkers may be low, making it important to develop highly sensitive immunoassays with the ability to detect

proteins at very low concentrations. Improving the limit of detection (LOD) would facilitate disease detection at early stages, and can help screen many diseases.

The traditional protein immunoassays are based on the antibody-antigen binding approaches, and one of the most well-established and commonly applied techniques is ELIZA. These antibody-based approaches rely on fluorogenic or chromogenic substrates for actual signal generation and the LOD is mostly in the ng/ml to pg/ml range. [32]

To further advance the sensitivity of protein detection in immunoassays, people have been developing signal amplification based on different approaches. Signal amplification can be achieved in either chemical or enzymatic systems, and common strategies for signal amplification include biotin-streptavidin system, chemical system, enzymatic amplification, and nucleic acid replication assisted exponential amplification [33]. In the following section the most powerful signal amplification mechanism, the immune-PCR assay, will be discussed.

The principle behind immune-PCR is to use oligonucleotide (ex. DNA or RNA) labeled antibodies instead of the most validated enzyme-linked antibodies for detection. This labeling strategy provides the advantages of exponential signal amplification power, which is derived from polymerase chain reaction. Nowadays, significant efforts have been spent on developing simple oligonucleotide labeling techniques on antibodies. With this advancement, the immune-PCR assays have been shown to be effective in detecting proteins with concentrations 10^2 to 10^5 fold lower than the conventional ELISA assays. These advancements of linking nucleic acids with existing antibody binding approach have brought LOD of protein immunoassay to another scale.[34] [35, 36]

1.4 Immunoassay platform

Immunoassays are used to quantify molecules of biological interest based on the specificity and selectivity of generated antibody reagents. Successful assay developments usually require validation of many variables such as analytes to test, detection mechanisms, availability of the testing instruments, sensitivity, throughput, and cost. While the choice of antibody or antigen is often related to detection dynamic range, sensitivity, and limit of detection, the design of the platform also deserves equal attention for optimal selection since it has a substantial effect on cost, availability, and throughput.

Various assay platforms have been explored for the detection and quantification of biologically important proteins. These platforms are designed to aim at different issues. These include an optical sensing microcantilever-based sensor, which shows very high sensitivity (0.2 ng/ml) [37], and a self-contained, colorimetric detecting paper-based microfluidic platform [38]. Other protein immunoassay platform such as bead-based flow cytometric assays with high throughput and antibody-array immunoassay have already been discussed above. The single-atom layer material, graphene, has also been explored of its potential in biosensing. Current development of graphene-based biosensors can be either electrical sensors or optical sensors. [39, 40]

1.5 Other goals

There are other emerging trends in immunoassay development. These include immunoassay automation to provide hands-free operation with the potential to gain productivity and save time; point-of-care diagnostic platform development for testing infectious diseases, cancer, and immune diseases; new assay platform application for improved performance; and miniaturization for portable assay systems.

1.6 Graphene in biosensing

Since 2004, the first discovery of graphene has added a new field of nanomaterials in biosensing research [41] Various nanomaterials, including nanoparticles, nanowires, carbon nano tubes (CNT) have been studied for their potential in biomolecule detection [42]. . The unique properties of graphene such as high surface-to-volume ratio, excellent electrical conductivity, good mechanical flexibility, and transparency have made graphene a promising candidate in biosensing.

Currently there are many methods of graphene production. These include chemical vapor deposition (CVD)-grown graphene, reduced graphene oxide (RGO), and exfoliation of graphite or graphite oxide. The feasibility of synthesizing graphene in different ways increases the opportunities for applying graphene in biosensing development. Graphene-based biosensing systems can be classified as the following: (I) electrical transducers such as field-effect-transistors, electrochemical biosensors, impedance biosensors (II) fluorescence biosensors [43].

Graphene exhibits good electronic properties with very high charge carrier mobilities [44], motivating people to apply its superior conductivity for various biomolecules sensing (ex.

glucose, DNA, proteins [45-47]) as bioelectronics devices [48]. The other direction that has also brought a lot of interest is to apply graphene in fluorescence biosensing. Graphene quenches fluorophores due to a fluorescence resonance energy transfer from dye to graphene. This quenching detection mechanism has been applied in thrombin detection, DNA sensing [49], and virus screening [50, 51].

1.7 Dissertation map

In this dissertation, the first chapter explores some fundamental characteristics of developing graphene as a protein biosensing platform. The work is specifically conducted on CVD graphene with the production availability of large size (> cm^2 scale). This development of graphene-based immunoassay platform is promising in fabricating a flexible, portable, and wearable biosensor/device.

The second chapter describes the application of microfluidic technique to protein immunoblotting. The design is aiming at improving current existing techniques with the goals of improving detection efficiency and reducing cost. In addition to improving protein screening and detection efficiency on the existing sensing platform, the microfluidic system has also been demonstrated to be applicable for inflammatory signaling pathway profiling.

The third chapter describes the application of microfluidics to dot blotting. In addition to showing the advantages of improving the efficiency and reducing reagent consumption, the device design constraints were also studied. Finally the results of using microfluidic dot blotting for cytokine detection were presented.

1.8 References

1. Grossman, H.B., et al., *Detection of bladder cancer using a point-of-care proteomic assay.* JAMA, 2005. **293**(7): p. 810-6.
2. Gstaiger, M. and R. Aebersold, *Applying mass spectrometry-based proteomics to genetics, genomics and network biology.* Nat Rev Genet, 2009. **10**(9): p. 617-27.
3. Pan, S., et al., *Mass spectrometry based targeted protein quantification: methods and applications.* J Proteome Res, 2009. **8**(2): p. 787-97.
4. Elshal, M.F. and J.P. McCoy, *Multiplex bead array assays: performance evaluation and comparison of sensitivity to ELISA.* Methods, 2006. **38**(4): p. 317-23.
5. Zhu, H. and M. Snyder, *Protein chip technology.* Curr Opin Chem Biol, 2003. **7**(1): p. 55-63.
6. Jun, B.H., et al., *Fluorescence-based multiplex protein detection using optically encoded microbeads.* Molecules, 2012. **17**(3): p. 2474-90.
7. Zhu, H. and M. Snyder, *Protein arrays and microarrays.* Curr Opin Chem Biol, 2001. **5**(1): p. 40-5.
8. Kodadek, T., *Protein microarrays: prospects and problems.* Chem Biol, 2001. **8**(2): p. 105-15.
9. Templin, M.F., et al., *Protein microarray technology.* Drug Discov Today, 2002. **7**(15): p. 815-22.
10. Wilson, D.S. and S. Nock, *Recent developments in protein microarray technology.* Angew Chem Int Ed Engl, 2003. **42**(5): p. 494-500.
11. Schena, M., et al., *Quantitative monitoring of gene expression patterns with a complementary DNA microarray.* Science, 1995. **270**(5235): p. 467-70.
12. Templin, M.F., et al., *Protein microarrays and multiplexed sandwich immunoassays: what beats the beads?* Comb Chem High Throughput Screen, 2004. **7**(3): p. 223-9.
13. Sydor, J.R. and S. Nock, *Protein expression profiling arrays: tools for the multiplexed high-throughput analysis of proteins.* Proteome Sci, 2003. **1**(1): p. 3.
14. Darwish, I.A., *Immunoassay Methods and their Applications in Pharmaceutical Analysis: Basic Methodology and Recent Advances.* Int J Biomed Sci, 2006. **2**(3): p. 217-35.
15. Cox, K.L., et al., *Immunoassay Methods*, in *Assay Guidance Manual*, G.S. Sittampalam, et al., Editors. 2004: Bethesda (MD).

16. Andreotti, P.E., et al., *Immunoassay of infectious agents.* Biotechniques, 2003. **35**(4): p. 850-9.
17. Sapin, R., *[Interferences in immunoassays: Mechanisms and outcomes in endocrinology]*. Ann Endocrinol (Paris), 2008. **69**(5): p. 415-25.
18. Deshpande, S.S., *Enzyme immunoassays : from concept to product development*. 1996, New York: Chapman & Hall. xiii, 464 p.
19. Nolan, J.P. and F. Mandy, *Multiplexed and microparticle-based analyses: quantitative tools for the large-scale analysis of biological systems.* Cytometry A, 2006. **69**(5): p. 318-25.
20. Hsu, H.Y., T.O. Joos, and H. Koga, *Multiplex microsphere-based flow cytometric platforms for protein analysis and their application in clinical proteomics - from assays to results.* Electrophoresis, 2009. **30**(23): p. 4008-19.
21. Krishhan, V.V., I.H. Khan, and P.A. Luciw, *Multiplexed microbead immunoassays by flow cytometry for molecular profiling: Basic concepts and proteomics applications.* Crit Rev Biotechnol, 2009. **29**(1): p. 29-43.
22. Breen, E.J., V. Polaskova, and A. Khan, *Bead-based multiplex immuno-assays for cytokines, chemokines, growth factors and other analytes: median fluorescence intensities versus their derived absolute concentration values for statistical analysis.* Cytokine, 2015. **71**(2): p. 188-98.
23. Hartmann, M., et al., *Protein microarrays for diagnostic assays.* Anal Bioanal Chem, 2009. **393**(5): p. 1407-16.
24. Wingren, C. and C.A. Borrebaeck, *Antibody-based microarrays.* Methods Mol Biol, 2009. **509**: p. 57-84.
25. Wilson, R., A.R. Cossins, and D.G. Spiller, *Encoded microcarriers for high-throughput multiplexed detection.* Angew Chem Int Ed Engl, 2006. **45**(37): p. 6104-17.
26. Wingren, C. and C.A. Borrebaeck, *Progress in miniaturization of protein arrays--a step closer to high-density nanoarrays.* Drug Discov Today, 2007. **12**(19-20): p. 813-9.
27. Haab, B.B., M.J. Dunham, and P.O. Brown, *Protein microarrays for highly parallel detection and quantitation of specific proteins and antibodies in complex solutions.* Genome Biol, 2001. **2**(2): p. RESEARCH0004.

28. MacBeath, G. and S.L. Schreiber, *Printing proteins as microarrays for high-throughput function determination.* Science, 2000. **289**(5485): p. 1760-3.
29. Angenendt, P., *Progress in protein and antibody microarray technology.* Drug Discov Today, 2005. **10**(7): p. 503-11.
30. Szurdoki, F., K.L. Michael, and D.R. Walt, *A duplexed microsphere-based fluorescent immunoassay.* Anal Biochem, 2001. **291**(2): p. 219-28.
31. Earley, M.C., et al., *Report from a workshop on multianalyte microsphere assays.* Cytometry, 2002. **50**(5): p. 239-42.
32. Dixit, C.K., et al., *Development of a high sensitivity rapid sandwich ELISA procedure and its comparison with the conventional approach.* Anal Chem, 2010. **82**(16): p. 7049-52.
33. Diamandis, E.P., *Analytical methodology for immunoassays and DNA hybridization assays--current status and selected systems--critical review.* Clin Chim Acta, 1990. **194**(1): p. 19-50.
34. Sano, T., C.L. Smith, and C.R. Cantor, *Immuno-PCR: very sensitive antigen detection by means of specific antibody-DNA conjugates.* Science, 1992. **258**(5079): p. 120-2.
35. Janssen, K.P., et al., *Nucleic acids for ultra-sensitive protein detection.* Sensors (Basel), 2013. **13**(1): p. 1353-84.
36. Wu, J., et al., *Biomedical and clinical applications of immunoassays and immunosensors for tumor markers.* Trac-Trends in Analytical Chemistry, 2007. **26**(7): p. 679-688.
37. Wu, G., et al., *Bioassay of prostate-specific antigen (PSA) using microcantilevers.* Nat Biotechnol, 2001. **19**(9): p. 856-60.
38. Ellerbee, A.K., et al., *Quantifying colorimetric assays in paper-based microfluidic devices by measuring the transmission of light through paper.* Anal Chem, 2009. **81**(20): p. 8447-52.
39. He, Y., et al., *Graphene oxide-based fluorescent biosensor for protein detection via terminal protection of small-molecule-linked DNA.* Small, 2013. **9**(12): p. 2097-101.
40. Heldt, C.L., et al., *Stacked graphene nanoplatelet paper sensor for protein detection.* Sensors and Actuators B-Chemical, 2013. **181**: p. 92-98.
41. Novoselov, K.S., et al., *Electric field effect in atomically thin carbon films.* Science, 2004. **306**(5696): p. 666-9.

42. Katz, E. and I. Willner, *Biomolecule-functionalized carbon nanotubes: applications in nanobioelectronics.* Chemphyschem, 2004. **5**(8): p. 1084-104.
43. Pumera, M., *Graphene in biosensing.* Materials Today, 2011. **14**(7-8): p. 308-315.
44. Bolotin, K.I., et al., *Temperature-dependent transport in suspended graphene.* Phys Rev Lett, 2008. **101**(9): p. 096802.
45. Kwak, Y.H., et al., *Flexible glucose sensor using CVD-grown graphene-based field effect transistor.* Biosens Bioelectron, 2012. **37**(1): p. 82-7.
46. Mohanty, N. and V. Berry, *Graphene-based single-bacterium resolution biodevice and DNA transistor: interfacing graphene derivatives with nanoscale and microscale biocomponents.* Nano Lett, 2008. **8**(12): p. 4469-76.
47. Ohno, Y., K. Maehashi, and K. Matsumoto, *Label-free biosensors based on aptamer-modified graphene field-effect transistors.* J Am Chem Soc, 2010. **132**(51): p. 18012-3.
48. Hess, L.H., M. Seifert, and J.A. Garrido, *Graphene Transistors for Bioelectronics.* Proceedings of the Ieee, 2013. **101**(7): p. 1780-1792.
49. He, S.J., et al., *A Graphene Nanoprobe for Rapid, Sensitive, and Multicolor Fluorescent DNA Analysis.* Advanced Functional Materials, 2010. **20**(3): p. 453-459.
50. Chang, H., et al., *Graphene fluorescence resonance energy transfer aptasensor for the thrombin detection.* Anal Chem, 2010. **82**(6): p. 2341-6.
51. Jung, J.H., et al., *A graphene oxide based immuno-biosensor for pathogen detection.* Angew Chem Int Ed Engl, 2010. **49**(33): p. 5708-11.

CHAPTER 2

FLUOROPHORE AND PROTEIN CONJUGATED DIELS-ALDER FUNCTIONALIZED CVD GRAPHENE LAYERS

Abstract

Chemical modification of the graphene web is emerging as a promising approach in band gap engineering of graphene devices and in producing solution-processable graphene derivatives for applications in electronics and nano/biotechnology. The zero-band-gap electronic structure of graphene has provided the opportunity to modify graphene by Diels-Alder chemistry via pairwise formation of sp^3 centers on the graphene lattice, thereby modifying the electronic, chemical and magnetic properties of graphene. Here we develop an approach to covalently attach fluorescent molecules to Diels-Alder modified CVD graphene to visualize the graphene layers, and to estimate the functional group density created by conjugating Alexa 488 cadaverine dye followed by XPS analysis. In addition, we demonstrate that proteins can be attached to graphene surface via the amine coupling reaction. Our present method provides an efficient way of visualizing graphene layers and provides an approach to the problem of estimating the density of functional groups on graphene surface.

2.1 Introduction

Graphene is a strictly two dimensional (2D) carbon membrane of atomic thickness that has enormous scientific and technological potential because of its high electrical and thermal conductivity, mobility of charge carriers, mechanical strength, and transparency.[1-3] Moreover, recent advances in graphene chemical functionalization have potential applications in many fields, including the development of biosensing platforms.[4-6] Chemical functionalization provides the capability of adding functional groups on the graphene surface in a controlled manner, which is crucial for the capture of targeted biomolecules in a sensing platform design,[4, 7] with previous work focusing on epitaxial graphene or graphene oxide.[8-10] Each of these methods has its own limitations compared to chemical vapor deposition (CVD) in terms of ease

of fabrication, scalability, and cost. Moreover, most methods for attaching biomolecules to the graphene surface are based on non-covalent binding, whereas covalent interaction is usually preferable in diagnostic applications to reduce concerns about interference from the heterogeneous mixtures of analytes.[11]

Covalent modification of the graphene surface with functional groups provides a means of covalently immobilizing most biomolecules including DNA, enzymes, peptides, and proteins.[10, 12-15] A functional group of particular interest is the carboxyl (-COOH) group. The synthetic utility of carboxylic acid functional groups coupling to other species through relatively simple chemistry such as amide or ester formation has been widely adopted in various techniques in such as surface plasmon resonance (SPR) and microarrays. It allows versatile biomolecules to be conjugated with stable, effective and high quality results.[16, 17]

Imaging graphene layers is important for characterization of the material; each technique for imaging has its own advantages and limitations, so new approaches to visualization of the layers are always desirable to complement existing methods. The gross macroscopic features of these atomically thick carbon membranes are often visualized on dielectric substrates (e.g. SiO_2/Si) by optical interference contrast.[18] For characterization at shorter length scales, atomic force microscopy (AFM), which scans materials with a tiny tip, is frequently used. AFM, however, is a slow process that can only look at small areas on smooth surfaces. Scanning electron microscopy (SEM) scans a surface with high-energy electrons, but only works if the material is placed in vacuum and is not particularly useful for characterizing chemical properties. Visualizing suspended graphene samples is extremely challenging, and often accomplished using SEM rather than optical techniques. Therefore, there are growing demands for developing new graphene imaging techniques.[19]

We have recently demonstrated that the unique zero-band-gap electronic structure of graphene together with its possession of high-lying HOMO (low ionization potential), low-lying LUMO (high electron affinity), and symmetries of the degenerate graphene frontier molecular orbitals (FMOs) at the Dirac point (K-point) facilitate the chemical behavior of graphene as a versatile Diels-Alder substrate.[20, 21] Indeed, the wide scope and versatility of the Diels-Alder

pericyclic reaction in organic chemistry could potentially enable covalent grafting of a wide range of diene and dienophile molecules with modifiable functionalities to graphene.

In this report, we establish a method of functionalizing CVD graphene and creating carboxylic acid groups (Gr-COOH) on the graphene surface. Graphene surface modification with the creation of carboxylic functional groups is accomplished by the synthetic method of the Diels-Alder reaction. In this reaction, graphene reacts as a diene with maleic anhydride, a dienophile, and this allows the maleic anhydride moiety to be grafted on graphene (MA-Gr), and subsequent hydrolysis generates free carboxylic acid groups (Gr-COOH). The Diels-Alder chemistry transforms a pair of neighboring sp^2 carbon bonds into sp^3 bonds. To characterize the functionalized graphene sheets, we have used Raman spectroscopy and X-ray photoelectron spectroscopy (XPS). We also estimate the functional group density created by conjugating Alexa 488 cadaverine dye followed by XPS analysis. Finally, we demonstrate that proteins can be covalently attached to graphene surface via EDC-NHS amine coupling reaction and we investigate the conjugation conditions by using fluorescence microscopy.

2.2 Materials and Methods

Materials and Instruments

Maleic anhydride (F.W. = 98.06), p-xylene, ammonium hydroxide (NH_4OH), N-(3-Dimethylaminopropyl)-N′-ethylcarbodiimide hydrochloride (EDC, 98+%, F.W. =191.71), *N*-Hydroxysuccinimide (NHS, F.W. =115.09), triethylamine (Et_3N, >99.5%, F.W.=101.19), ammonium persulfate were obtained from Sigma-Aldrich. Bovine Serum Albumin (BSA protein), Fraction V, Heat Shock Treated were obtained from Fisher Scientific. Alexa Fluor 488 Cadaverine, Sodium Salt (F.W. =640.61) and Alexa Fluor 488 Carboxylic acid, Succinimidyl Ester (F.W. =643.41) were obtained from Life Technologies. 950PMMA A4 resist was obtained from MicroChem Corporation.

Preparation of CVD Graphene Samples

CVD-grown single layer graphene (SLG) samples were either purchased from Bluestone Global Tech or grown at Michigan using standard CVD techniques. During the CVD process, the graphene was synthesized on 25 μm thick copper foil (99.8%, Alfa Aesar), which was loaded into an inner quartz tube inside a 3 inch horizontal tube furnace of a commercial CVD system

(First Nano EasyTube 3000). The system was purged with argon gas and evacuated to a vacuum of 0.1 Torr. The sample was then heated to 1000°C in H_2 (100 sccm) environment with a vacuum level of 0.35 Torr. When 1000 °C is reached, 70 sccm of CH_4 is flowed for 15 minutes at a vacuum level of 0.45 Torr. The sample was then allowed to cool slowly to room temperature. The vacuum level was maintained at 0.5 Torr with 100 sccm of argon gas flowing during cooling. SLG on copper surface, thus grown, was characterized by use of Raman spectroscopy.

Diels-Alder Chemistry of CVD Graphene

In a typical reaction, CVD graphene on a copper substrate was placed inside a round-bottom flask; a solution of maleic anhydride (MA, ~0.05 M in p-xylene) was added and then flushed with argon. The solution was heated at 120-125 ^oC under argon atmosphere for 20 hrs. The system was allowed to cool down to room temperature, washed with acetone, and then with isopropanol to obtain Diels-Alder modified graphene, MA-Gr. The reaction was monitored with Raman spectroscopy.

Hydrolysis of the Grafted Functionalities

The Diels-Alder adduct of MA and CVD graphene was hydrolyzed by heating MA-Gr with ammonium hydroxide solution at 50 ^oC for 5 min, then washed with copious amounts of distilled water, then rinsed with absolute ethanol, and finally dried under gentle flow if argon.

Conjugation of the Fluorescent Dye, Alexa Fluor 488 by EDC/NHS Coupling Reaction

The carboxylic acid groups on the functionalized graphene sample were coupled with amine (-NH_2) groups on the fluorophores through the EDC/NHS coupling reaction.

In the reaction EDC (0.4 M) and NHS (0.4 M) were dissolved in water and added to cover the whole surface of graphene on copper foil. The sample in solution was placed on a shaker and reacted for 2 hours. Once the reaction was completed, the sample was removed and washed in DI water. Afterwards, it was immediately placed in the solution with the fluorescent dye. To conjugate fluorophores on the graphene surface, a solution of 1 mg of Alexa Fluor 488 Cadaverine, sodium salt in 400 µl water (0.004 M) with 2µl of Et_3N was prepared and added to the previously treated graphene sample. The sample was reacted for two hours then washed with DI water. Finally, the sample was dried in a lyophilizer overnight.

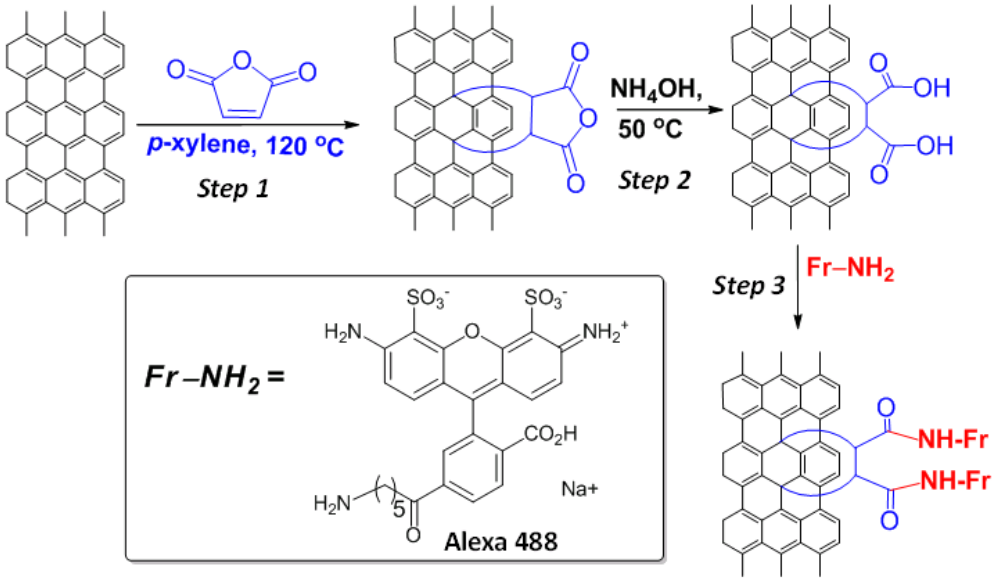

Scheme 2.1. Procedures for graphene functionalization.

Step 1: Diels-Alder chemistry of CVD grown graphene (as a diene) on copper substrates with a dienophile (maleic anhydride; MA) to obtain MA-Gr adduct. ***Step 2***: Hydrolysis of the adduct to form free carboxylic acid moieties on graphene surface (Gr-COOH). ***Step 3***: Conjugation of Alexa 488 fluorophore with Gr-COOH via amide linkage.

XPS Spectroscopy of graphene samples

Prior to X-ray photoelectron spectroscopic (XPS) analysis, the functionalized graphene samples were mounted onto standard sample stubs and secured by washers. The samples were mounted on the holder by adhesive copper tape (3M). XPS measurements were performed using Kratos Axis Ultra XPS spectrometer with a monochromated Al X-ray source. XPS analysis was carried out in an ultra-high-vacuum chamber equipped with a fast-entry introductory chamber. Prior to analysis, all samples were evacuated in the introductory chamber using a turbo-molecular pump for at least 90 min to ensure low vacuum. Samples were then introduced into the XPS analysis chamber (P_{base} < 1 x 10^{-8} Torr). XP spectra were recorded using the X-ray irradiation from an aluminum (Al) anode at 14 kV and 300 W. Elemental scans were acquired using a pass energy of 20 eV and a resolution of 0.125 eV/step. Binding energies were referenced to the C 1s peak at 284.8 eV.

The survey scans of XPS spectrum of Alexa-488 cadaverine conjugated CVD graphene on copper foil were obtained. The photo electron binding energies covering in the range from 0 to 600 eV are present, together with 30 eV width narrow scans for C(1s) and N(1s) elements that are present for the quantitative analysis. Integration of the narrow-scan peak areas, after linear

background subtraction, enables elemental surface atomic percentages to be calculated, using manufacture supplied relative sensitivity factors ; C 1s (1), O 1**s** (2.93), and N 1s (1.8).

Fluorescence Visualization

After graphene functionalization was completed, the surface was spin-coated with 950PMMA A4 (Microchem) resist and cured at 180 °C for 5 minutes. (As a result, the PMMA layer is on top of the functional groups.) The sample was then left in ammonium persulfate (Sigma Aldrich) solution (0.03 g/mL) for at least 12 hours to completely dissolve away the copper layer. The sample was transferred onto a glass slide and dried overnight. Functionalized graphene was then be visualized under a fluorescence microscope (Olympus).

2.3 Results and Discussion

Fabrication of Diels-Alder Modified CVD Graphene

The functionalization of graphene using maleic anhydride (MA) under Diels-Alder reaction has been reported previously, and this reaction allows maleic anhydride moieties to be grafted onto graphene surface (MA-Gr)[20, 21]. Here we further hydrolyze maleic anhydride to create carboxylic acid functional groups on the graphene surface by using ammonium hydroxide (NH_4OH). For the synthesis work, the maleic anhydride was grafted onto graphene surface and subsequently hydrolyzed with ammonium hydroxide to obtain the product, Gr-COOH.

The covalent functionalization of CVD graphene, which occurs with the saturation of conjugated sp^2-hybridized atoms converted to sp^3, was confirmed and characterized by Raman spectroscopy. Figure 2.1 shows the Raman spectra of (a) CVD graphene, (b) Gr-MA, and (c) Gr-COOH. The Raman spectrum of the starting material CVD graphene shows two characteristic peaks of graphene, the G-band (~ 1583 cm^{-1}) and the 2D band (~ 2680 cm^{-1}). After DA chemistry, there is a transformation of the sp^2 carbon atoms in the graphene honeycomb lattice to sp^3 atoms and this results in the creation of D-band (~ 1350 cm^{-1}) in Raman spectrum, which can be clearly seen in the spectra of Gr-MA (I_D/I_G = 0.4) and Gr-COOH (I_D/I_G = 0.5).

After conjugation of the Alexa 488 fluorophore, the Raman spectrum of Gr-CONH-Fr (Gr-Alexa 488 cadaverine in Scheme 1, step 3) was not very informative due to the overwhelming fluorescence background contribution from the Alexa 488 fluorophore dye. After conjugation of Alexa 488 dye, the overall signals (Raman intensity) are much higher after the coupling reaction than the one before the coupling reaction when scanned with the 514 nm excitation laser.

Consequently, with the 514 nm laser excitation the spectrum showed fully saturated signals with no distinguishable peaks.

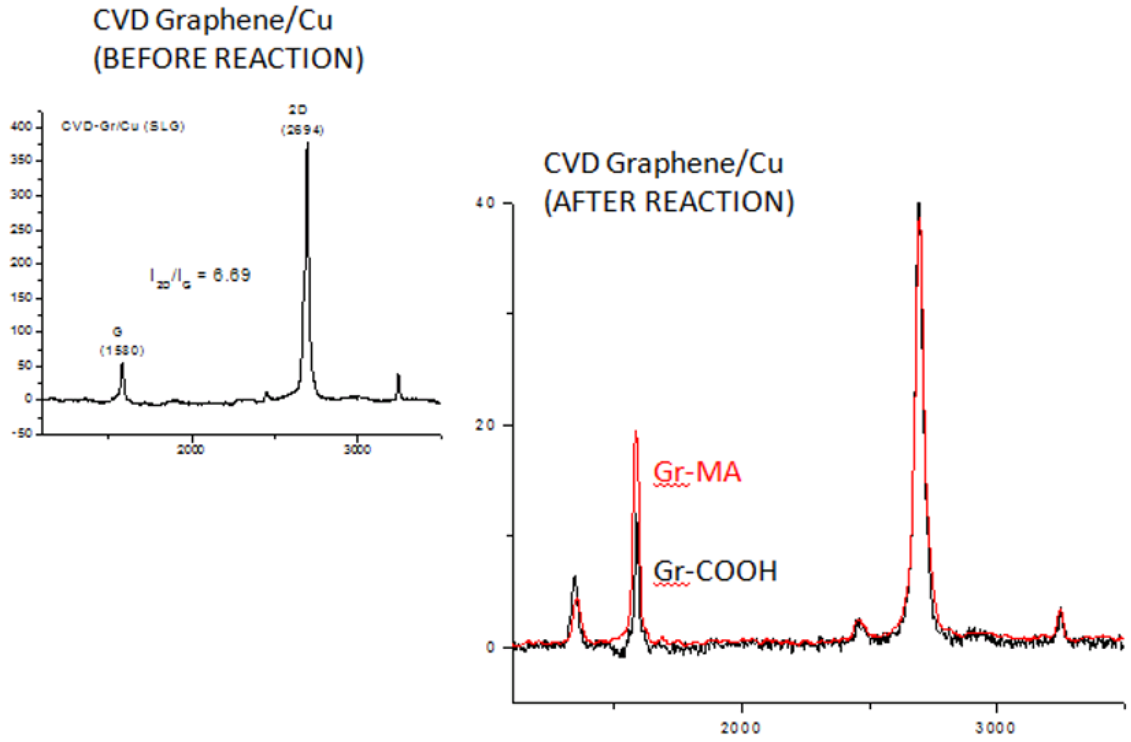

Figure 2.1. Raman spectroscopy of graphene.

Raman spectroscopy of (a) pristine CVD graphene (CVD Gr) on copper substrate, (b) Diels-Alder modified CVD graphene, MA-Gr adduct, and (c) the product of hydrolysis, Gr-COOH.

Conjugation of Alexa 488 cadaverine to Gr-COOH

After the hydrolysis step (**Scheme 1, step 2**), carboxylates (-COOH) are created on the functionalized graphene surface. The -COOH functional groups can be applied in the amine coupling reaction through 1-Ethyl-3-[3-dimethylaminopropyl] carbodiimide (EDC)/N-hydroxysulfosuccinimide (NHS)-mediated approach (**Scheme 1, step 3**). We verified the coupling reaction by conjugating Alexa 488 cadaverine to the functionalized graphene, where both reactions (-COOH functional group creation and EDC-NHS coupling reaction) proceeded with the CVD graphene on the copper substrate. The conjugation of fluorophores makes possible the visualization of the graphene sheet via fluorescence microscopy when the fluorophore-conjugated graphene layer is transferred from the copper foil to a transparent substrate such as a glass slide. A common method for CVD-grown graphene transfer uses a polymer layer such as PMMA,[22] so functionalized graphene on copper foil was first coated with a PMMA support

layer. PMMA is a polymer which is transparent and does not yield auto-fluorescence (Figure 2.7 (Appendix)), so coating it on top of the functionality on the graphene sheet does not interfere with the fluorescence from the Alexa 488 dye conjugated on the graphene surface. Once PMMA was coated on the functionalized graphene, the copper foil was dissolved in ammonium persulfate and the graphene with PMMA layer was transferred to a glass slide. Figure 2.2 and Figure 2.5 (Appendix) show the image of a graphene sheet with PMMA coated and imaged by fluorescence microscopy. In the example shown in Figure 2.2, the sample unintentionally folded during the transfer process. We observe that the folded graphene layers do not quench the fluorescence, and the fluorescence yield is approximately linear with the number of layers.

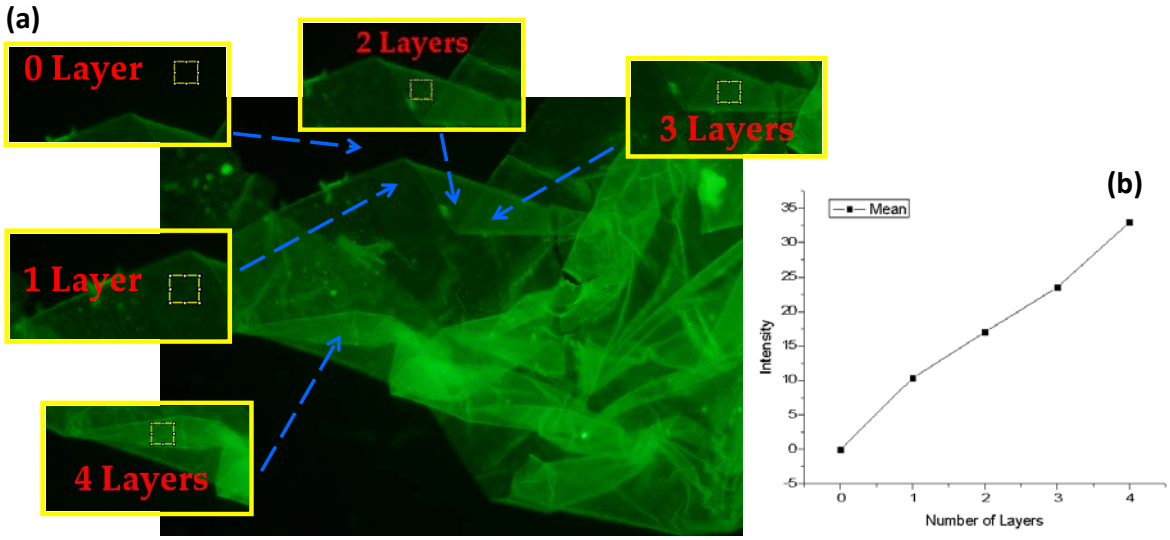

Figure 2.2. Fluorescence images of Alexa 488 cadaverine conjugated graphene. (a) Functionalized graphene conjugated with Alexa 488 (coated with PMMA) imaging by fluorescence microscopy. The transfer process of PMMA coated graphene sheet to the glass slide without copper substrate caused the graphene sheet edges to fold (not intentionally). Fluorescent signals were quantified at regions which the number of layers can be identified. (b) Mean values of the fluorescence intensity from different number of graphene layers using ImageJ. Signal from empty area (0 layer) was subtracted as background noise.

We also observe that the optical distribution of the conjugated fluorophore is highly uniform, and this implies the carboxylic acid functional groups are created uniformly on the graphene surface. Since we can not calibrate the absolute fluorescence efficiency of the conjugated dye, it is not possible to extract the dye surface density directly from the fluorescence; it is possible, however,

to estimate the density of the carboxylic acid functional groups (-COOH) on the graphene surface by using XPS.

XPS Analysis of Functionalized Graphene Samples

X-ray photoelectron spectroscopy (XPS) is a technique that provides information of surface element composition, materials' electronic and structural information. Figure 2.3 shows the XPS spectrum of CVD graphene and DA-functionalized graphene conjugated with Alexa 488 cadaverine.

The C 1s spectra confirm the results from Raman spectroscopy that functionalization has been achieved successfully. As seen in Figure 2.3, the carbon C 1s peak, observed at 284.4 eV for sp^2 pristine carbon, shifts as expected to the higher binding energy of ~ 284.9 eV after Diels-Alder surface modification.[23] This further verifies the creation of sp^3 bond by opening the double bond and the C-C bond formation after the functionalization.

Besides the demonstration of fluorescence from fluorophores conjugated to DA-functionalized graphene, the conjugation of Alexa 488 cadaverine can also be used as XPS labels for carboxylic groups existed on the DA-functionalized graphene surface. The XPS spectra provide information of the amounts of material in the sample surface since the integrated peak areas can be used for the quantification of the elemental atomic percentages.[24]

Since the fluorescent dye molecules Alexa 488 attach specifically to the -COOH functional groups, measuring the N 1s spectral emission of the Alexa 488 fluorescent dye allows the identification and quantification of the -COOH functional groups on the graphene surface. The percentage of the elemental surface composition corresponding to the carboxyl groups can be derived using XPS via the emission from the N 1s level of the label. From the XPS survey spectrum of CVD graphene and DA-functionalized graphene sheets, both samples show the C 1s peaks, but only the functionalized sample shows a N 1s signal at 398.95 eV binding energy. The remaining signals can be assigned to oxygen, whose core level electrons have a binding energy of 530 eV, Cu 3s, Cu 3p and Auger lines. The copper signal arises from the copper foil beneath graphene.

The ratio of the C 1s peak area to the N 1s peak area, or the C/N ratio, provides an estimation of the density of the -COOH functional groups on the graphene surface. Since nitrogen is absent from the native graphene surface, the coupling reaction of fluorescent dye Alexa 488 cadaverine

to the carboxylic functional groups (-COOH) provides nitrogen atoms attached to the graphene surface. This information can be used to quantify the density of the carboxylic functional groups (-COOH) on the surface by measuring the C/N element ratio as shown in the Supporting Information. Table 1 details the surface element composition for CVD graphene and DA-functionalized graphene conjugated with Alexa 488.

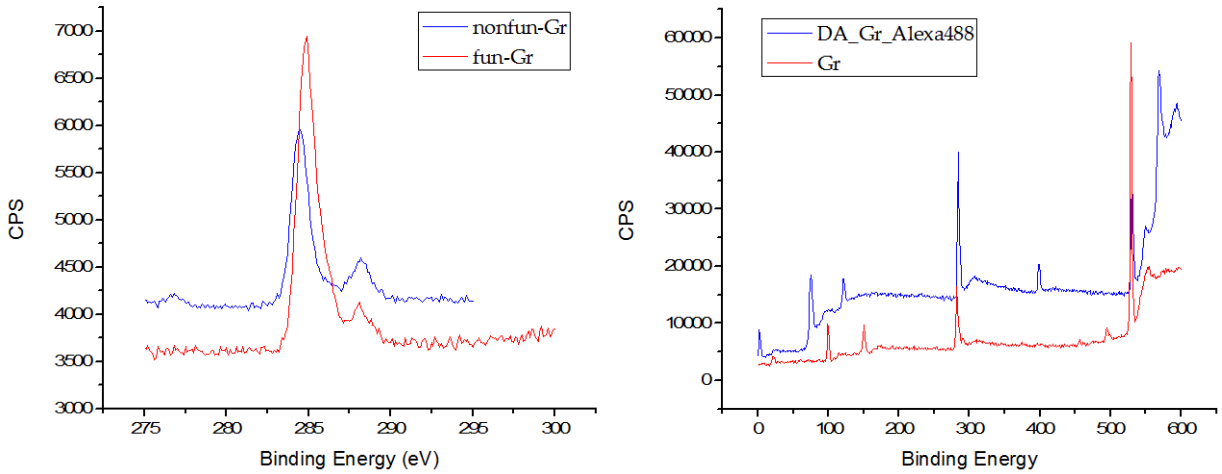

Figure 2.3. The XPS spectra of pristine CVD graphene and DA-functionalized graphene conjugated with Alexa 488 cadaverine (a) C 1s spectra (b) Survey scan (0-600 eV).

Table 2.1. The percentage elemental composition of CVD graphene and DA-functionalized graphene surfaces determined using XPS.

Material	% C	% O	% N	Coverage of carboxyl groups on the graphene surface as a percentage of the elemental composition (%)
CVD Graphene (pristine)	91.73	8.27	--	Undetermined
DA-functionalized graphene with Alexa 488 cadaverine	70.05	21.02	8.93	71.61

Protein Immobilization of Diels-Alder modified CVD graphene

To investigate the potential for developing the graphene surface with carboxylic functional groups as a biosensing platform, we conjugated a model protein (fluorescein isothiocyanate-labeled BSA) to a chemically modified graphene surface. It is apparent from Figure 2.4 that

conjugation of BSA-Alexa 488 with Diels-Alder modified graphene (Gr-COOH) leads to visualization of graphene basal planes and graphene edges [Figure 2.4(a)] by fluorescence microscopy. In sharp contrast to this covalent conjugation of BSA-Alexa 488 with graphene, non-covalent binding or adsorption of the same BSA-Alexa 488 with pristine CVD graphene (no Diels-Alder modified graphene) does not lead to visualization of graphene layers [Figure 2.4(c)], indicating the absence of adsorption.

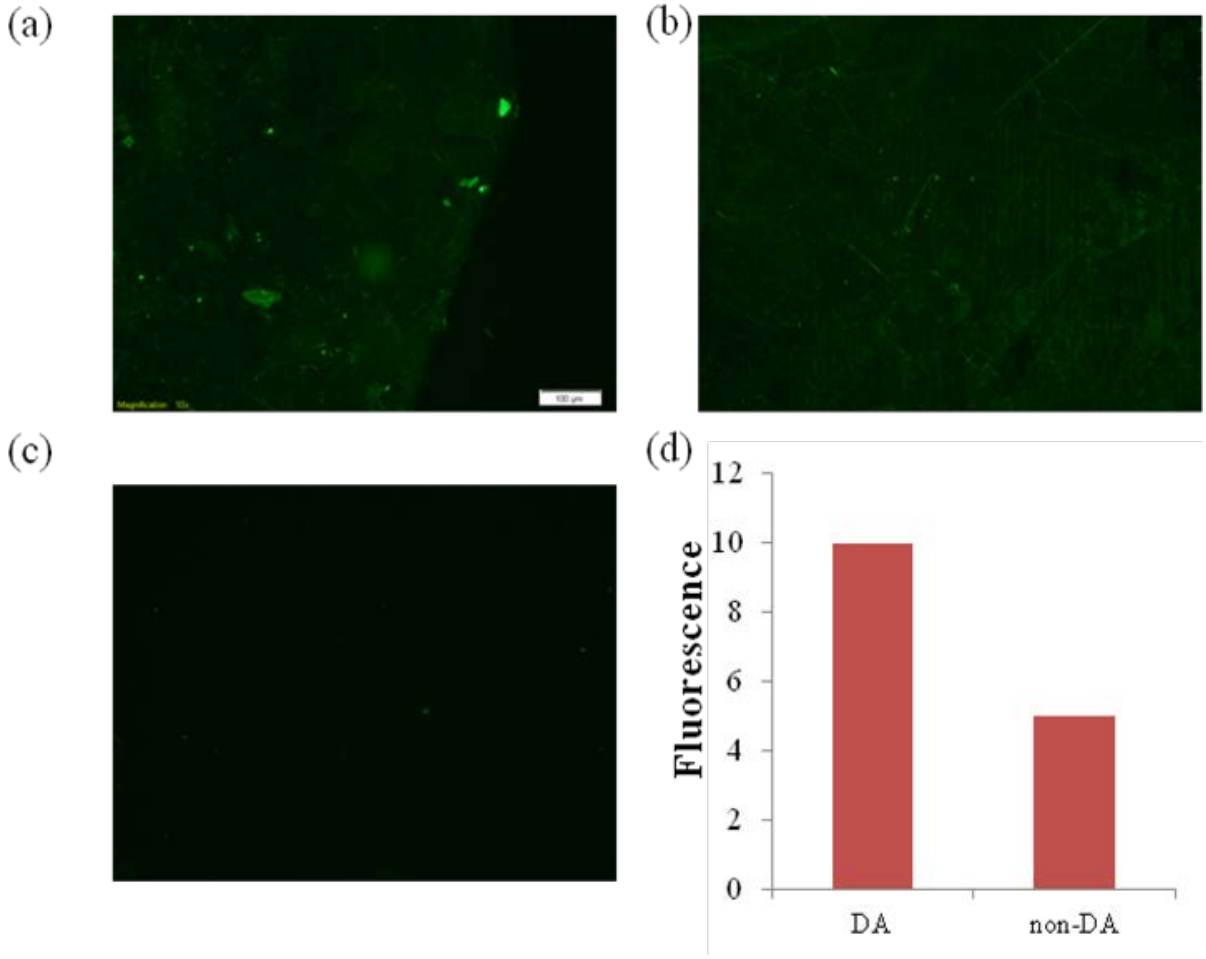

Figure 2.4. Fluorescence images of BSA conjugated graphene. (a) Functionalized graphene conjugated with BSA-Alexa 488 (coated with PMMA) imaging by fluorescence microscopy at the edge and (b) at the center. (c) Fluorescent microscopy image of BSA-Alexa 488 conjugation with pristine CVD graphene (non-covalent adsorption) at the center. (d) Comparison of fluorescence intensity of samples in (b) and (c).

2.4 Conclusions

In the present article, we employ the versatile Diels-Alder reactivity of graphene as a diene by its reaction with maleic anhydride (a dienophile) to graft the maleic anhydride moiety to graphene (MA-Gr), which upon hydrolysis generates free carboxylic acid groups (Gr-COOH). The versatile nature of the carboxylic acid functionality enables its coupling with a wide range of moieties with the amine ($-NH_2$), alcohol (-OH), ester (-COOR) etc. terminals. Here we employ the conjugation of the Alexa 488 fluorophore with amine terminal with G-COOH through an amide (-CONH) linkage, which makes quick visualization and identification of different number of graphene layers feasible. Finally, we demonstrate that proteins can be covalently attached to graphene surface via EDC-NHS amine coupling reaction and we investigate the conjugation condition by using fluorescence microscopy. Our present method of graphene biosensor development with different biomolecule immobilization techniques may enable easy and high throughput visualization of graphene layers, and could lead to accurate estimates of the surface coverage of functional groups. Thus our present approach solves important challenges in graphene research including the imaging and visualization of graphene layers, and estimating density of functional groups on graphene surface.

Appendix

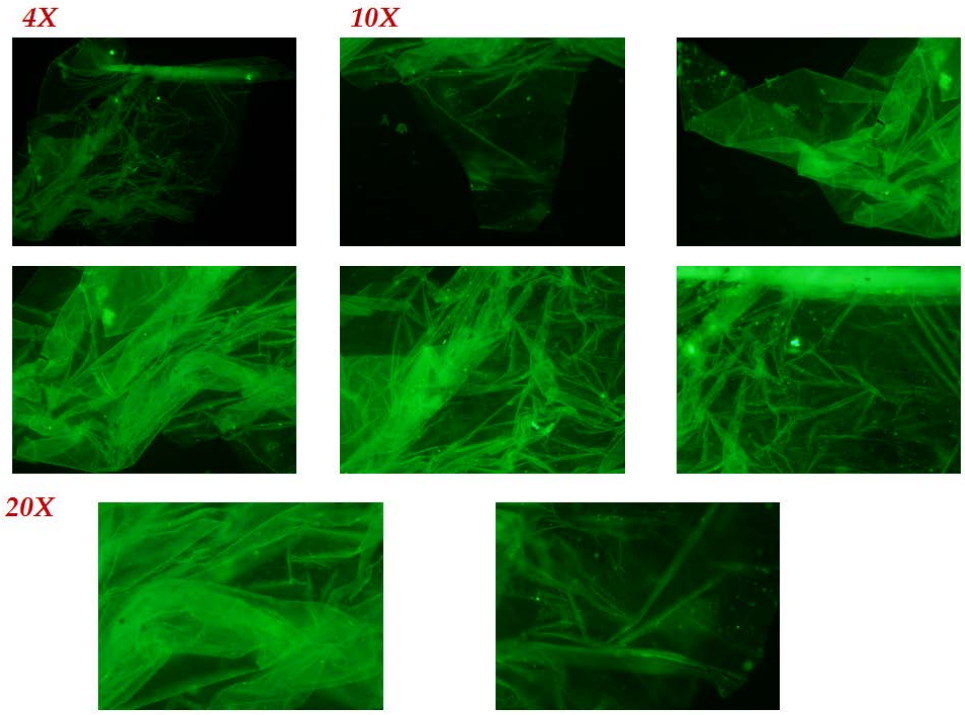

Figure 2.5. Alexa 488 cadaverine conjugated to Diels-Alder reaction functionalized graphene visualized under fluorescence microscopy

Synthesis of Fluorescent Dye Labeled Proteins and the Conjugation to Graphene Surface

BSA protein was first labeled with the fluorescent dye Alexa 488 carboxylic acid succinimidyl ester by linking the succinimidyl esters to the primary amines on BSA. In the reaction, BSA (0.5mM) and Alexa 488 carboxylic acid succinimidyl ester (1.5mM) were dissolved in water and added in Et_3N (2.25mM) and stirred for reaction for 2 hours. The reaction steps were carried out in glass flasks at room temperature.

The protein solution mixture was purified using 10K MWCO centrifugal filtration devices (Amicon Ultra-4). Purification consisted of five cycles using 1X PBS and five cycles using DI water. All cycles were 15 minutes at 4000 rpm. The resulting product was lyophilized overnight to yield a yellow solid. Sample's molecular weight is characterized by MALDI-TOF mass spectroscopy with the result 67358.

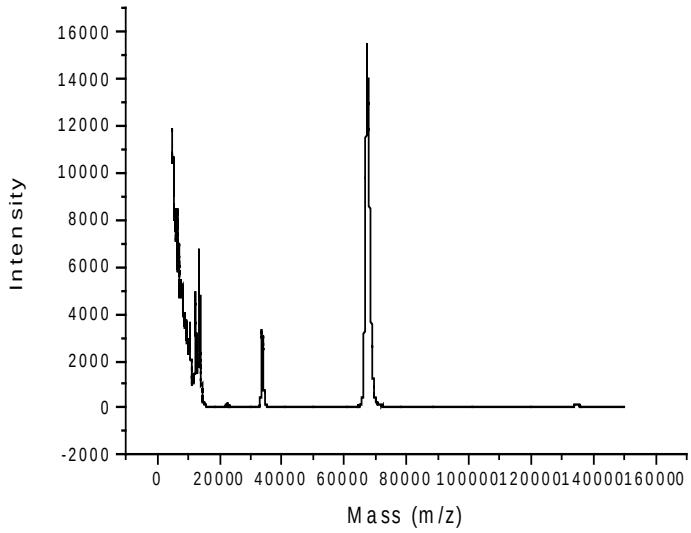

Figure 2.6. MALDI-TOF mass spectroscopy characterization of BSA proteins conjugated with Alexa 488 carboxylic acid, succinimidyl ester.

Conjugation of the Fluorescent Dye labeled proteins to DA functionalized graphene surface

The carboxylic acid groups on the functionalized graphene sample are coupled with amine ($-NH_2$) groups on the BSA proteins through EDC/NHS coupling reaction.

In the reaction EDC (0.4 M) and NHS (0.4 M) were dissolved in water and added to cover the whole surface of graphene on copper foil. The sample in solution was placed on a shaker and reacted for 2 hours. Once the reaction is completed, the sample was removed and washed in DI water. Afterwards, it was immediately placed in the solution with the fluorescent dye-labeled BSA proteins. To conjugate fluorophores on graphene surface, solution of 8mg of Alexa 488 carboxylic acid succinimidyl ester conjugated BSA was dissolved in 800 µl water with 2µl of Et_3N was prepared and added to the previously treated graphene sample. The sample was reacted for two hours then washed with DI water. Finally, the sample was dried in a lyophilizer overnight.

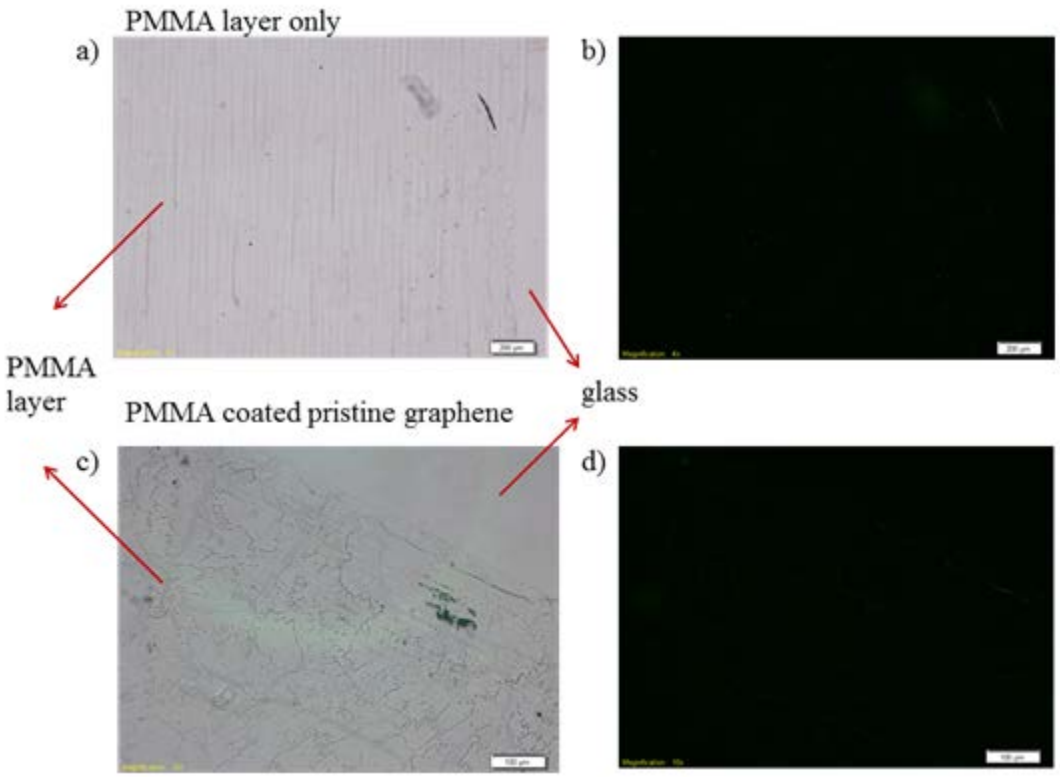

Figure 2.7. PMMA layer and pristine graphene visualized under optical microscopy and fluorescence microscopy. (a) PMMA layer under optical microscopy. (b) PMMA layer under fluorescence microscopy. (c) PMMA layer coated pristine graphene under optical microscopy. (d) PMMA layer coated pristine graphene under fluorescence microscopy.

XPS quantification

$$Gr - COOH + C_{26}H_{25}N_4O_{10}S_2Na \rightarrow Gr - CONH - C_{26}N_3O_{10}S_2Na \quad \text{(S1)}$$

If we use the expression, $[C]_0$ and $[O]_0$ are the initial concentrations of C and O present on the surface as determined by XPS and $[O]_0^{COOH}$ is the surface concentration of carboxylic acid groups. The above equation gives equation S2

$$[N] = \frac{2\varepsilon[O]_0^{COOH}}{[C]_0+[O]_0+21\times\varepsilon[O]_0^{COOH}} \qquad \text{(S2)}$$

So,

$$[C]_0[N] + [O]_0[N] + 21\varepsilon[O]_0^{COOH}[N] = 2\varepsilon\,[O]_0^{COOH}$$

$$[C]_0[N] + [O]_0[N] = (2\varepsilon - 21\varepsilon[N])[O]_0^{COOH}$$

and

$$\%[O]_0^{COOH} = \frac{[C]_0[N] + [O]_0[N]}{2\varepsilon - 21\varepsilon[N]} \times 100 \qquad (S3)$$

This equation can be used to determine the concentration of carboxylic acid groups on the functionalized graphene surface, so

If reaction S1 proceeds with 100% efficiency (i.e. $\varepsilon = 1$), then

$$\%[O]_0^{COOH} = \frac{[C]_0[N] + [O]_0[N]}{2 - 21[N]} \times 100 \qquad (S3)$$

2.5 Referenes

1. Novoselov, K.S., et al., *A roadmap for graphene.* Nature, 2012. **490**(7419): p. 192-200.
2. Berger, C., et al., *Ultrathin epitaxial graphite: 2D electron gas properties and a route toward graphene-based nanoelectronics.* Journal of Physical Chemistry B, 2004. **108**(52): p. 19912-19916.
3. Sarkar, S., E. Bekyarova, and R.C. Haddon, *Covalent chemistry in graphene electronics.* Materials Today, 2012. **15**(6): p. 276-285.
4. Kasry, A., et al., *Detection of Biomolecules via Benign Surface Modification of Graphene.* Chemistry of Materials, 2011. **23**(22): p. 4879-4881.
5. Yang, W.R., et al., *Carbon Nanomaterials in Biosensors: Should You Use Nanotubes or Graphene?* Angewandte Chemie-International Edition, 2010. **49**(12): p. 2114-2138.
6. Pumera, M., *Graphene in biosensing.* Materials Today, 2011. **14**(7-8): p. 308-315.
7. Georgakilas, V. and Wiley Online Library (Online service), *Functionalization of graphene*. p. 1 online resource (426 pages).
8. Kodali, V.K., et al., *Nonperturbative Chemical Modification of Graphene for Protein Micropatterning.* Langmuir, 2011. **27**(3): p. 863-865.
9. Liu, Y., et al., *Biocompatible graphene oxide-based glucose biosensors.* Langmuir, 2010. **26**(9): p. 6158-60.
10. Shen, J.F., et al., *Covalent attaching protein to graphene oxide via diimide-activated amidation.* Colloids and Surfaces B-Biointerfaces, 2010. **81**(2): p. 434-438.
11. Jiang, K.Y., et al., *Protein immobilization on carbon nanotubes via a two-step process of diimide-activated amidation.* Journal of Materials Chemistry, 2004. **14**(1): p. 37-39.
12. Shen, J.F., et al., *Synthesis of graphene oxide-based biocomposites through diimide-activated amidation.* Journal of Colloid and Interface Science, 2011. **356**(2): p. 543-549.
13. Hu, X.G., et al., *Immobilized smart RNA on graphene oxide nanosheets to specifically recognize and adsorb trace peptide toxins in drinking water.* Journal of Hazardous Materials, 2012. **213**: p. 387-392.
14. Bonanni, A., A. Ambrosi, and M. Pumera, *Nucleic Acid Functionalized Graphene for Biosensing.* Chemistry-a European Journal, 2012. **18**(6): p. 1668-1673.
15. Liu, Y., et al., *Biocompatible Graphene Oxide-Based Glucose Biosensors.* Langmuir, 2010. **26**(9): p. 6158-6160.

16. Lens, J.P., et al., *Introduction of carboxylate groups at poly(ethylene) surfaces by argon plasma immobilization of sodium salts of fatty acids.* Langmuir, 1997. **13**(26): p. 7052-7062.
17. Zammatteo, N., et al., *Comparison between different strategies of covalent attachment of DNA to glass surfaces to build DNA microarrays.* Analytical Biochemistry, 2000. **280**(1): p. 143-150.
18. Novoselov, K.S., et al., *Two-dimensional atomic crystals.* Proceedings of the National Academy of Sciences of the United States of America, 2005. **102**(30): p. 10451-10453.
19. Kim, J., et al., *Visualizing Graphene Based Sheets by Fluorescence Quenching Microscopy.* Journal of the American Chemical Society, 2010. **132**(1): p. 260-267.
20. Sarkar, S., E. Bekyarova, and R.C. Haddon, *Chemistry at the Dirac Point: Diels-Alder Reactivity of Graphene.* Accounts of Chemical Research, 2012. **45**(4): p. 673-682.
21. Sarkar, S., et al., *Diels-Alder chemistry of graphite and graphene: graphene as diene and dienophile.* J Am Chem Soc, 2011. **133**(10): p. 3324-7.
22. Pirkle, A., et al., *The effect of chemical residues on the physical and electrical properties of chemical vapor deposited graphene transferred to SiO2.* Applied Physics Letters, 2011. **99**(12).
23. Lee, Y.S., et al., *Surface properties of fluorinated single-walled carbon nanotubes.* Journal of Fluorine Chemistry, 2003. **120**(2): p. 99-104.
24. Denison, P., F.R. Jones, and J.F. Watts, *The Use of Xps and Labeling Techniques to Study the Surface-Chemistry of Carbon-Fibers.* Journal of Physics D-Applied Physics, 1987. **20**(3): p. 306-310.

Chapter 3

PROFILING INFLAMMATORY RESPONSES WITH MICROFLUIDIC IMMUNOBLOTTING

Abstract

Rapid profiling of signaling pathways has been a long sought after goal in biological sciences and clinical medicine. To understand these signaling pathways, their protein components must be profiled. The protein components of signaling pathways are typically profiled with protein immunoblotting. Protein immunoblotting is a powerful technique but has several limitations including the large sample requirements, high amounts of antibody, and limitations in assay throughput. To overcome some of these limitations, we have designed a microfluidic protein immunoblotting device to profile multiple signaling pathways simultaneously. We show the utility of this approach by profiling inflammatory signaling pathways (NFκB, JAK-STAT, and MAPK) in cell models and human samples. The microfluidic immunoblotting device can profile proteins and protein modifications with 5380-fold less antibody compared to traditional protein immunoblotting. Additionally, this microfluidic device interfaces with commonly available immunoblotting equipment, has the ability to multiplex, and is compatible with several protein detection methodologies. We anticipate that this microfluidic device will complement existing techniques and is well suited for life science applications.

3.1 Introduction

Inflammation is now recognized as a driver of several chronic diseases including cancer and heart disease [1,2]. Although many regulatory steps are involved, protein modifications are one of the defining features of inflammatory responses [3-5]. Since its inception in 1979, protein immunoblotting has become the standard technique for profiling proteins and protein modifications in molecular biology and clinical diagnostics [6]. Although traditional protein

immunoblotting is a powerful technique, it has several limitations including its slow throughput, the requirement for relatively large sample and antibody amounts, and the inability to probe for multiple proteins simultaneously [7]. As our recognition of the role of inflammation in disease has grown, there is a need for more robust approaches to monitor the signaling pathways that drive inflammation. To overcome some of the limitations of traditional protein immunoblotting, several variations have been introduced including membrane stripping and the use of fluorescent secondary antibodies. Despite their improvements, these variations have their own limitations, including loss of signal intensity and increased assay variability. Additionally, none of these variations address the large sample and antibody amounts required by traditional protein immunoblotting. Recently, microfluidic technology has been applied to molecular biology and in clinical diagnostics. The small volumes and spatial control afforded by microfluidics make it an exciting complement to existing technologies. With regards to protein immunoblotting, microfluidic immunoblotting devices have been fabricated with most approaches trying to integrate all aspects of protein immunoblotting. The Herr group has recently presented several approaches that incorporate microfluidic technology with traditional protein immunoblotting [8,9]. Their approaches are significant improvements over existing immunoblotting platforms because of the integration of all aspects of protein immunoblotting [10]. Pan and colleagues made advances by introducing a fluorescence based microfluidic immunoblotting device that could detect several proteins and is compatible with existing protein immunoblotting technologies [11]. We wished to build upon these advancements without sacrificing the accuracy and accessibility of traditional protein immunoblotting. We fabricated a microfluidic device that can simultaneously profile multiple proteins using existing immunoblotting equipment and chemiluminescent detection technologies. We demonstrate the utility of this microfluidic device by monitoring several inflammatory signaling pathways in culture models and human samples.

3.2 Materials and Methods

Microfluidic protein immunoblotting

The transparency mask was printed using a CAD file of the microfluidic device (CAD/Art Services, Inc.; Bandon, OR USA). Soft-lithography was used to fabricate a silicon master mold from the transparency mask. The microfluidic devices were created by mixing the pre-polymer and curing agent (Sylgard 184 Silicone Elastomer Kit, Dow Corning; Midland, MI USA) and

then pouring on to the silicon master. After gel electrophoresis, the gels were electroblotted onto a PVDF membrane (Life Technologies; Carlsbad, CA USA) for 1 hour at 30V. The PVDF membrane was dried overnight before proceeding to microfluidic immunoblotting. The microfluidic assembly was created by sandwiching the PVDF membrane between a glass support and the PDMS microfluidic device. The PDMS microfluidic device was aligned to the ladder to ensure accurate channel placement over the sample lanes. To complete the assembly, two glass slides were placed on top of the PDMS device for further support. The spacing between the two glass slides was approximately 0.5mm and was used as the injection site. The activating and antibody solutions were injected using a 1ml syringe with 27G ½ needles. The PVDF membrane was activated through the microfluidic channels using a 0.1% BSA and 0.1% Tween20 in TBS. Primary antibodies were injected through the microfluidic channels and incubated for 1 hour. Both the primary and secondary antibody dilutions were prepared in 0.1% BSA and 0.1% Tween20 TBS. Following the primary antibody incubation period, the microfluidic device was removed and the membrane was washed, blocked for 1 hour in 0.1% BSA and 0.1% Tween20 TBS, and then stained with the secondary antibody for 1 hour prior to chemiluminescent detection with either alkaline phosphatase or horseradish peroxidase.

Gel electrophoresis and protein immunoblotting

PBMCs were isolated using BD Vacutainer CPT Cell Preparation Tubes with Sodium Citrate. Following isolation, PBMC lysates were collected as described below. The murine macrophage cell line (RAW264.7) was purchased from American Type Culture Collection (ATCC; Manassas, VA USA) and cultured in RPMI medium (Life Technologies; Carlsbad, CA USA) supplemented with penicillin (100 U/ml), streptomycin (100 µg/ml) and 10% fetal bovine serum (Invitrogen) at a density of 3.0 X 106 . After the cells were allowed to adhere for 4 to 6 hours, the media was changed to RPMI media supplemented with 0.5% FBS, penicillin (100 U/ml), streptomycin (100 µg/ml), and incubated overnight (14-18 h). Endotoxin stimulation was initiated by incubating cells in 0.5% FBS medium containing lipopolysaccharide (LPS) from Escherichia coli O55:B5 (Sigma-Aldridge; St Louis, MO USA) at a concentration of 100 ng/ml. Cells were then harvested and lysed using RIPA buffer containing 25 mM Tris-HCl, pH 7.6, 150 mM NaCl, 1% Nonidet P-40, 1% sodium deoxycholate, 1 mM Na3VO4 , and 10 mM NaF (phosphatase inhibitors) and 0.1% SDS with 10 µl of Halt Protease Inhibitor Cocktail (Pierce; Rockford, IL USA) added for each 1 ml of buffer. Samples were separated using SDS-PAGE electrophoresis and transferred to

a PVDF membrane. PVDF membranes were probed with rabbit primary antibodies against active-JNK (phospho-JNK1/2; Promega; Madison, WI), active-MAPK (phospho-ERK; Promega), and ERK-1 (Santa Cruz Biotechnology; Santa Cruz, CA USA), NF-κB p65 (Cell Signaling Technology; Beverly, MA USA), STAT3 (sc-483, Santa Cruz Biotechnology; Santa Cruz, CA USA), and phospho-STAT3 (Cell Signaling Technology; Beverly, MA USA). Horseradish peroxidase (HRP) or alkaline phosphatase (AP) goat anti-rabbit secondary antibodies (Thermo Scientific; Rockford, IL USA) were used at a dilution of 1:20000.

Quantification and statistical analysis of protein immunoblots

Immunoblots were scanned and converted to 2400 dpi images. The images were imported into ImageJ software and analyzed as described below. For the traditional protein immunoblots, the signal intensity inside three boxes overlaying the band of interest was measured (each box was 10 pixels x 28 pixels); the average of these measurements was the signal intensity assigned to the band. The standard deviation of the signal intensity inside the three boxes was on average 9.9%. For the microfluidic protein immunoblots, the signal intensity of overlaying the region of interest was measured (each box was 10 pixels x 28 pixels). For both traditional and microfluidic immunoblots, the signal intensity was normalized to the signal intensity from the 5 μg of protein probed with the 1:1000 dilution of P65 antibody. Traditional and microfluidic immunoblots are representative of at least three independent protein immunoblots. Signal quantification is expressed as means with standard deviations (SD) with numbers of individual experiments presented in figure legends. Significance was tested using analysis of variance (ANOVA) with Newman–Keuls post hoc test ($P<0.05$).

3.3 Results and Discussion

Design and interface of the microfluidic device

The poly(dimethysiloxane) (PDMS) microfluidic device was designed to interface with existing immunoblotting equipment. The devices were fabricated using standard soft-lithography techniques as previously described [12].First, the transparency mask was printed from a CAD file of the microfluidic device. Soft-lithography was used to fabricate a silicon master mold from the transparency mask. The microfluidic device consisted of 5 lanes corresponding to the protein lanes of a traditional protein gel. Each lane contained 3 microfluidic channels (3.1 cm long, 150 μM wide, 100 μM deep). The microfluidic devices were created on the silicon master by mixing

the pre-polymer and curing agent at a mass ratio of 12:1. The microfluidic device was degassed and cured at 60° C for 1 hour. Our microfluidic immunoblotting approach consists of three stages including gel electrophoresis, transfer to a PVDF membrane, and microfluidic immunoblotting for proteins of interest (Figure 3.1). Because the first two stages are similar to traditional immunoblotting, the microfluidic device easily interfaces with existing immunoblotting equipment. After the samples were separated and transferred to the PVDF membrane, the PVDF membrane was placed between a glass support and the microfluidic device. The PVDF membrane was activated by filling and incubating the microfluidic channel with blocking solution for 20 minutes. After the PVDF membrane was activated, the microfluidic channels were filled with the

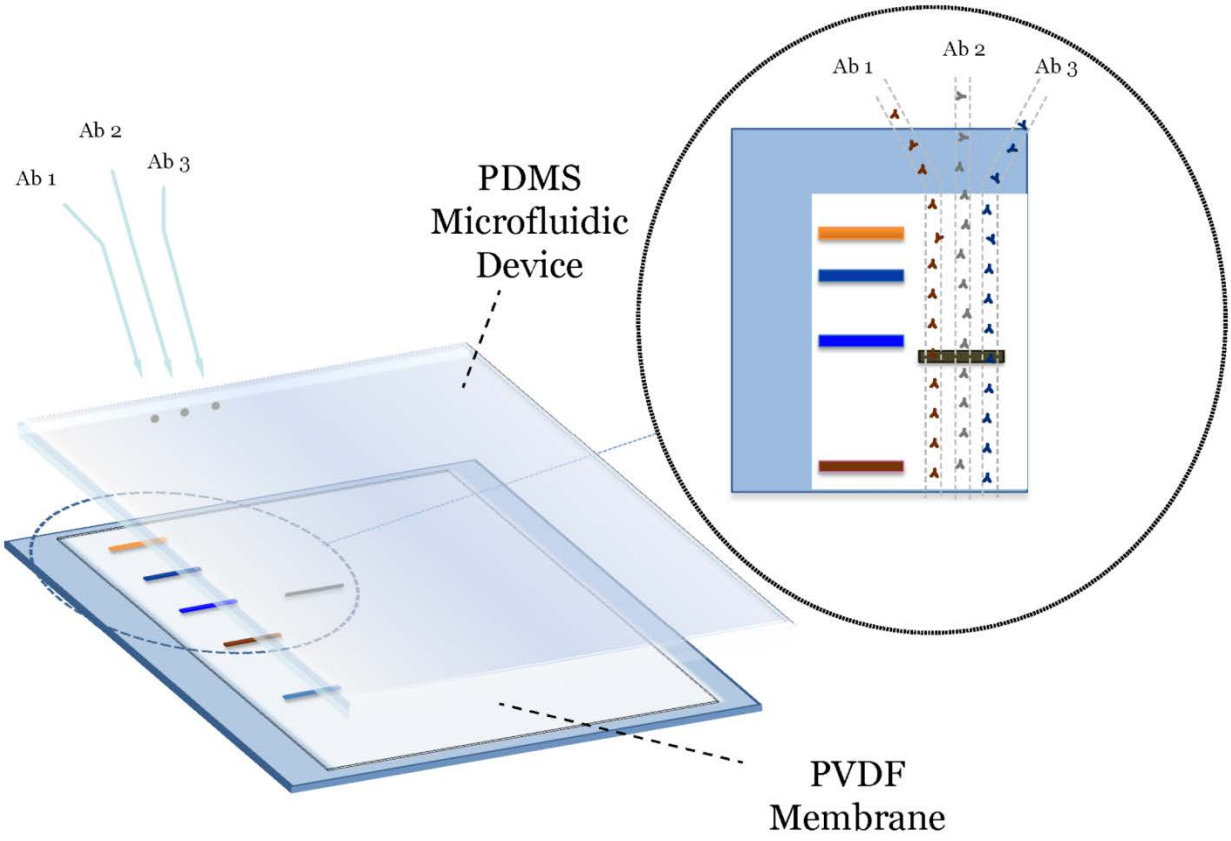

Figure 3.1. Schematic of a PDMS microfluidic device and the interface with a PVDF membrane. Microfluidic channels overlie each sample lane that can be used to probe for multiple proteins within each sample lane.

primary antibody and incubated for 1 hour. The microfluidic device was then removed and the PVDF membrane was washed. To detect the primary antibody, the entire PVDF membrane was incubated with the chemiluminescent secondary antibody and detected with the specified chemiluminescent substrates.

Comparison of traditional and microfluidic immunoblotting

We wished to compare the test characteristics of microfluidic immunoblotting with traditional immunoblotting. We collected peripheral blood monocytes (PBMC) from healthy volunteers and isolated protein lysates. Four different protein amounts were separated using gel electrophoresis and then transferred to a PVDF membrane. Using a primary antibody to RelA/p65, a member of the NF-κB transcriptional family, we compared the signals between microfluidic and traditional immunoblotting at three different primary antibody dilutions and the different protein loading amounts (Figure 3.2 and Figure 3.5 (Appendix)). The microfluidic immunoblotting approach resulted in slightly lower, but comparable signal intensities compared to those from

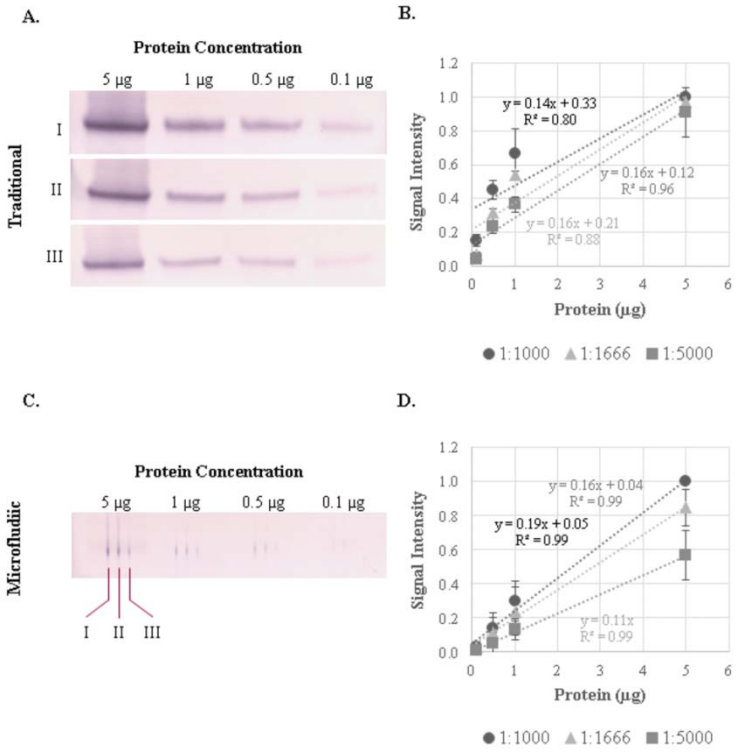

Figure 3.2. Comparison of traditional and microfluidic immunoblotting in human blood monocyte samples.

Representative immunoblots for RelA/p65 at four protein concentrations (5, 1, 0.5 and 0.1 µg) and three antibody dilutions (I: 1:1000; II: 1:1666; III: 1:5000) using (A) traditional and (B) microfluidic immunoblotting techniques. The signal intensity for the (C) traditional and (D) microfluidic blots were quantified using ImageJ software and normalized to the signal associated with 5 µg of protein probed with the 1:1000 p65 antibody dilution. Immunoblots are representative of three independent PVDF membranes from the same PBMC lysates.

traditional immunoblotting. In both approaches, the signals and signal variation were comparable under the conditions tested. For the PVDF membranes used in these experiments, a traditional immunoblotting assay for a single protein requires approximately 10 mL of primary antibody solution. Based on the microfluidic channel (0.015, 0.010, and 3.100 cm), approximately 0.000465 mL of primary antibody solution is required for each microfluidic channel. Using the microfluidic device, to assay a PVDF membrane for 1 protein requires 0.00186 mL of primary antibody solution (4 lanes *0.000465 mL of antibody/lane = 0.00186 mL primary antibody solution). Even without considering the multiplexing capacity of the microfluidic device, this translates into a 5380-fold reduction in primary antibody amounts compared with traditional protein immunoblotting. The implication of these results is that the microfluidic approach requires substantially less protein and antibody amounts to generate immunoblots of comparable quality. To further demonstrate the multiplexing ability of this approach, we fabricated a microfluidic device comprised of 5 channels per lane that performs similarly to the 3-channel microfluidic device (Figure 3.6 (Appendix)). For these reasons, microfluidic immunoblotting is ideally suited to profile signaling pathways from human samples and other low-protein samples.

Monitoring inflammatory pathway activation and protein modifications

Inflammatory pathways are often regulated through posttranslational modifications of signaling proteins [13,14]. Monitoring these posttranslational modifications is critical to capture the dynamics of inflammatory responses. Like the NFκB protein family, the signal transducer and activator of transcription (STAT) protein family coordinates many aspects of inflammatory responses [15]. In response to specific cytokines and growth factors, STAT family members are phosphorylated by receptor-associated kinases [16,17]. Protein phosphorylation, a common posttranslational modification, is typically monitored with protein immunoblotting. Because this type of posttranslational modification must be evaluated in the context of the total protein amount, both the phosphorylated and total protein levels must be profiled in parallel. These types of profiling experiments are well suited for microfluidic immunoblotting because the

phosphorylated and total protein can be profiled at the same time from the same sample lane. To evaluate this capacity of microfluidic immunoblotting, we stimulated RAW264.7 cells, a macrophage cell line, with lipopolysaccharide (LPS) (100 ng/ml) for 24 hours. After 24 hours, the cell lysates were collected and probed for phosphoSTAT3 and STAT3 with both microfluidic and traditional protein immunoblotting. Similar to traditional immunoblotting, microfluidic immunoblotting detected phospho-STAT3 in LPS stimulated macrophages consistent with inflammatory activation of the STAT pathway (Figure 3.3). These results suggest that microfluidic immunoblotting can be used to monitor phosphorylation and other posttranslational modifications. Importantly, the ability to monitor multiple proteins and protein modifications greatly improves assay throughput and reduces sample requirements without sacrificing data fidelity.

Monitoring multicomponent, inflammatory pathways

The mitogen activated protein kinase (MAPK) pathway is another pathway that coordinates inflammatory responses [18]. MAPKs are serine/threonine-specific protein kinases that transduce extracellular signals and regulate diverse cellular responses including cell proliferation, differentiation, and apoptosis. One of the difficulties in monitoring this pathway is that it has multiple protein components with different activation properties. These complexities make monitoring the MAPK pathway with traditional immunoblotting time and resource intensive. We hypothesized that some of these complexities could be addressed using microfluidic immunoblotting. To determine the efficacy of the microfluidic device to monitor the MAPK pathway, we stimulated RAW264.7 cells with LPS (100 ng/ml) for 45 minutes and collected cell lysates. We probed for phospho-JNK, phospho-ERK, and total ERK with traditional and microfluidic protein immunoblotting (Figure 3.4). Traditional immunoblotting required three different gels and PVDF membranes. In contrast, microfluidic immunoblotting obtained similar results using only two sample lanes from a single gel and PVDF membrane. By simultaneously probing for total ERK from the same sample, we minimized the time and resources compared with traditional immunoblotting. We also wanted to evaluate the flexibility of the microfluidic immunoblotting approach with other common chemiluminescent detection methods. Both HRP and AP have excellent sensitivity. However, this higher sensitivity also makes them more susceptible to background noise. We ran a microfluidic immunoblot using the same cell lysates and MAPK antibodies as above. We then used a horseradish peroxidase secondary antibody and

substrate to detect the primary antibodies. The efficacy of HRP detection was equivalent to alkaline phosphatase detection using the microfluidic immunoblotting device (Figure 3.4) further expanding the utility of this approach.

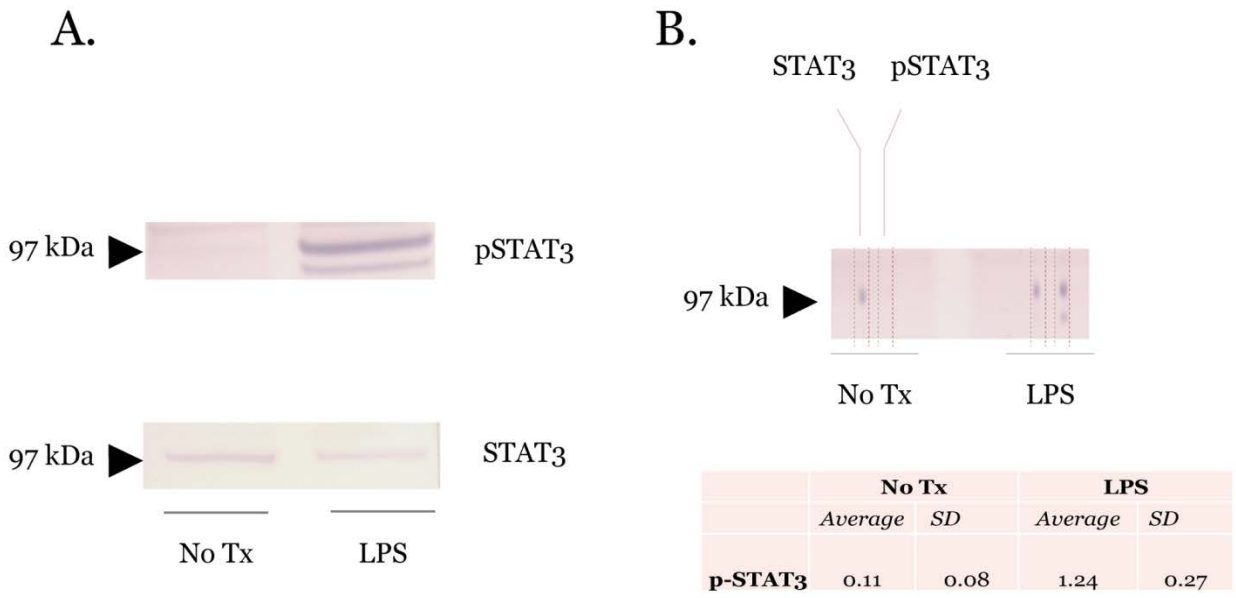

	No Tx		LPS	
	Average	*SD*	*Average*	*SD*
p-STAT3	0.11	0.08	1.24	0.27

Figure 3.3. Detection of STAT3 phosphorylation in response to inflammatory stimuli.

(A) Traditional immunoblots of RAW264.7 cell lysates showing phosphorylation of STAT3 in response to LPS stimulation. (B) Microfluidic immunoblot on same RAW264.7 cell lysates as (A). The signal intensities from three microfluidic immunoblots were quantified using ImageJ and demonstrate a robust and reproducible signal intensity. The microfluidic device allows for simultaneous monitoring of phospho-STAT3 and STAT3 in the same sample without the need for stripping or reprobing of the PVDF membrane. Immunoblots are representative of at least three independent PVDF membranes.

3.4 Conclusions

In this study, we report the design and evaluation of a microfluidic immunoblotting device to profile inflammatory responses. This approach is unique compared with previously described microfluidic immunoblotting platforms in that it: (1) easily interfaces with conventional protein immunoblotting platforms and can be used with several detection modalities, (2) can detect endogenous proteins and protein modifications from research and human samples, and (3) greatly reduces resource (antibody and sample) requirements and enhances assay throughput. Generally, microfluidic immunoblotting approaches can be categorized into two types: those that focus on integrating all of the elements of immunoblotting and those that focus on applying

microfluidics only to specific phases of immunoblotting. The former group of microfluidic platforms has obvious advantages and represents the ultimate goal of microfluidic immunoblotting platforms[19–22]. As mentioned above, Herr and colleagues have presented several microfluidic platforms integrating the separation, transfer, and detection steps of protein immunoblotting within a single device. Their methods are fast and enable simultaneous monitoring of several proteins. However, the immediate accessibility to typical molecular biology users may be limited since their focus is on automation and integration of immunoblotting steps. Ciaccio et al. recently presented an approach to monitor EGF receptor signaling using microwestern arrays [23]. Their technique captures the throughput advantages of microarray technology with the detection ability of traditional immunoblotting. This approach is clearly an advance, but does require specialized equipment and extensive sample processing. Although microfluidic integration of all the traditional immunoblotting elements is the desired goal, achieving this goal requires advances in microfluidics that also must surpass the ease and reproducibility of existing technologies. An intermediate goal is to use microfluidics for only some elements of protein immunoblotting. This goal has the advantages of greater flexibility and minimal end-user investment. However, to realize these advantages, the microfluidic device must be simple, reproducible, and easily interface with the existing immunoblotting technologies and equipment. Our microfluidic approach most closely resembles that of Pan and colleagues and focuses on integrating microfluidics with the detection phase of protein immunoblotting [11]. Although both approaches use a microfluidic device that interfaces with slab gels, there are several important differences. First, to reduce the complexity of the device, we used a low-volume syringe to load the microfluidic channels to obviate the need for pumps and tubing. Second, to improve the detection limits of our microfluidic device, we used chemiluminescent detection methodologies because of the increased sensitivity compared with fluorescent detection methodologies. Although the increased sensitivity improves detection limits, it requires a microfluidic platform with no leaking and a high degree of stability to maintain a low background signal. Lastly, in contrast to the microfluidic approach by Pan and colleagues, our approach resulted in primary antibody concentrations similar to those of traditional protein immunoblotting leading to greater reductions in primary antibody requirements. In conclusion, we have presented the design and evaluation of a microfluidic immunoblotting device for rapid profiling of inflammatory signaling pathways. The design of the microfluidic device allows for

the addition of more microfluidic channels that would further increase the amount of proteins that can be simultaneously profiled. The microfluidic approach maintains the data fidelity of traditional protein immunoblotting but greatly improves assay throughput and reduces resource requirements. Additionally, this approach is still compatible with membrane stripping and other PVDF membrane manipulations allowing for further microfluidic profiling of proteins. We anticipate that this microfluidic immunoblotting device will have utility in molecular biology and clinical diagnostics.

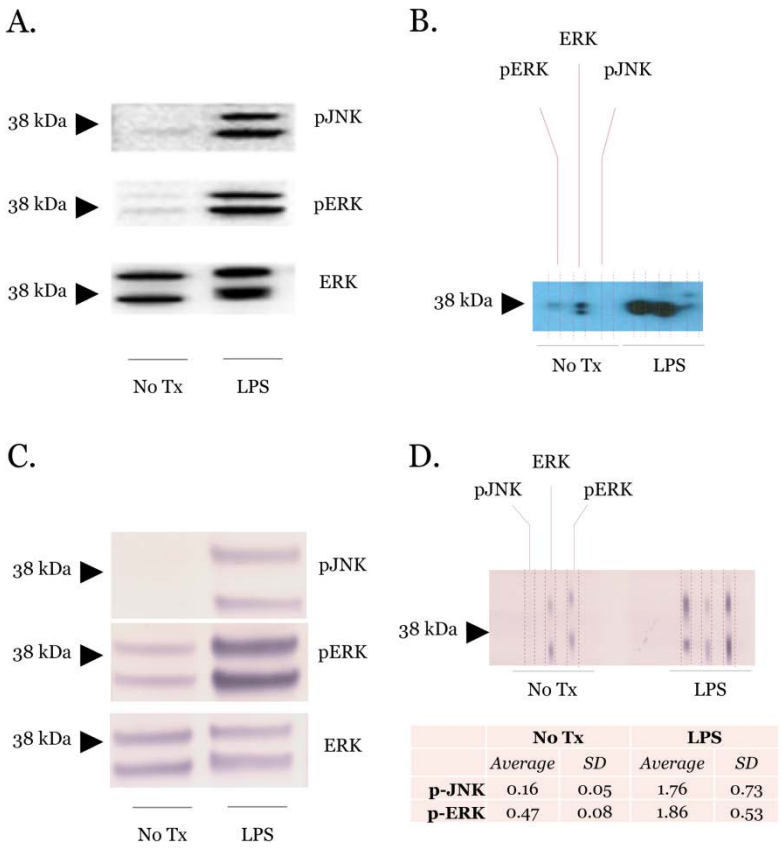

	No Tx		LPS	
	Average	*SD*	*Average*	*SD*
p-JNK	0.16	0.05	1.76	0.73
p-ERK	0.47	0.08	1.86	0.53

Figure 3.4. Protein immunoblots of the MAPK pathway using different chemiluminescent detection modalities.

(A) Traditional immunoblots of RAW264.7 cell lysates with or without LPS for 45 minutes. Membranes were probed for phospho-JNK and phospho-ERK using total ERK as the loading control. Primary antibodies were detected using HRP chemiluminescent techniques. (B) Microfluidic immunoblots mirroring conditions in (A). (C) and (D) are identical to (A) and (B) except they were performed using AP chemiluminescent secondary antibodies to detect primary antibodies. The signal intensities from three microfluidic immunoblots were quantified using ImageJ. Immunoblots are representative of at least three independent PVDF membranes.

Appendix

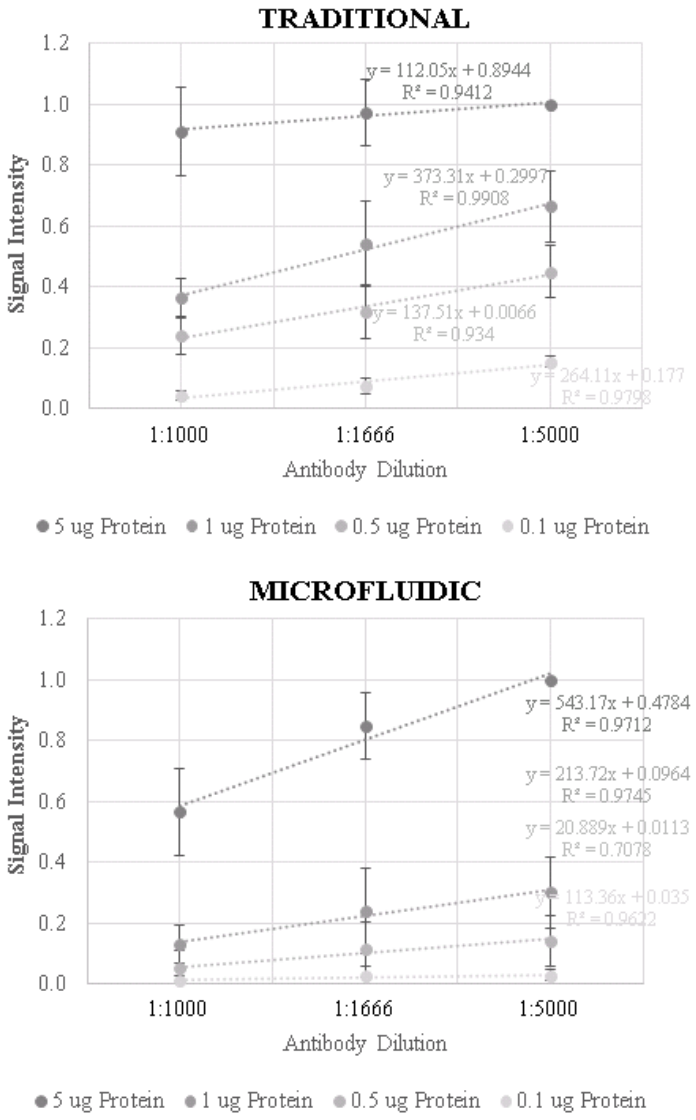

Figure 3.5. **Comparison of antibody and protein signal dependence of traditional and microfluidic protein immunoblotting.** Immunoblots from PBMCs were run and processed as described in the Materials and Methods section. Data are from three independent PBMC immunoblots (from the same sample) for RelA/p65 at four protein concentrations (5, 1, 0.5 and 0.1 µg) and three antibody dilutions. The normalized signal intensities represent measurements from 3 independent immunoblots. Under the conditions tested, the signal intensity was more dependent on protein concentration than on antibody concentration for both traditional and microfluidic protein immunoblotting.

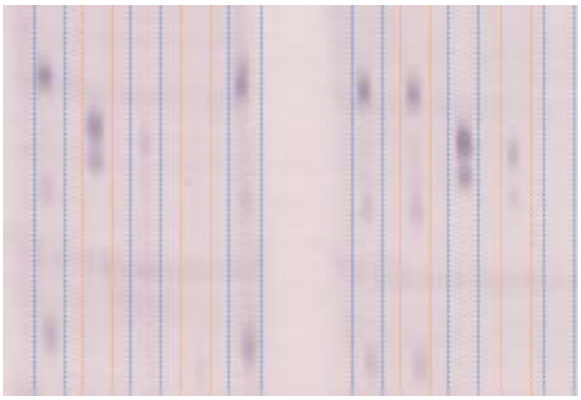

Figure 3.6. Example of microfluidic protein immunoblot generated using a 5-channel per lane microfluidic device.

3.5 References

1. Saleh M, Trinchieri G (2011) Innate immune mechanisms of colitis and colitis-associated colorectal cancer. Nat Rev Immunol 11: 9-20. PubMed: 21151034.

2. Hansson GK (2005) Inflammation, atherosclerosis, and coronary artery disease. N Engl J Med 352: 1685-1695. doi:10.1056/NEJMra043430. PubMed: 15843671.

3. Anderson P (2010) Post-transcriptional regulons coordinate the initiation and resolution of inflammation. Nat Rev Immunol 10: 24-35. doi:10.1038/nri2685. PubMed: 20029446.

4. Anderson P (2008) Post-transcriptional control of cytokine production. Nat Immunol 9: 353-359. doi:10.1038/ni1584. PubMed: 18349815.

5. Akira S, Takeda K (2004) Toll-like receptor signalling. Nat Rev Immunol 4: 499-511. doi:10.1038/nri1391. PubMed: 15229469.

6. Towbin H, Staehelin T, Gordon J (1979) Electrophoretic transfer of proteins from polyacrylamide gels to nitrocellulose sheets: procedure and some applications. Proc Natl Acad Sci U S A 76: 4350-4354. doi: 10.1073/pnas.76.9.4350. PubMed: 388439.

7. Wu Y, Li Q, Chen XZ (2007) Detecting protein-protein interactions by Far western blotting. Nat Protoc 2: 3278-3284. doi:10.1038/nprot. 2007.459. PubMed: 18079728.

8. He M, Herr AE (2009) Microfluidic polyacrylamide gel electrophoresis with in situ immunoblotting for native protein analysis. Anal Chem 81: 8177-8184. doi:10.1021/ac901392u. PubMed: 19731927.

9. Hughes AJ, Herr AE (2012) Microfluidic Western blotting. Proc Natl Acad Sci U S A 109: 21450-21455. doi:10.1073/pnas.1207754110. PubMed: 23223527.

10. Tia SQ, He M, Kim D, Herr AE (2011) Multianalyte On-Chip Native Western Blotting. Anal Chem, 83: 3581–8. PubMed: 21456518.

11. Pan W, Chen W, Jiang X (2010) Microfluidic Western blot. Anal Chem 82: 3974-3976. doi:10.1021/ac1000493. PubMed: 20426486.

12. Wu H, Odom TW, Chiu DT, Whitesides GM (2003) Fabrication of complex three-dimensional microchannel systems in PDMS. J Am Chem Soc 125: 554-559. doi:10.1021/ja021045y. PubMed: 12517171.

13. Medzhitov R (2008) Origin and physiological roles of inflammation. Nature 454: 428-435. doi:10.1038/nature07201. PubMed: 18650913.

14. Medzhitov R (2010) Inflammation 2010: new adventures of an old flame. Cell 140: 771-776. doi:10.1016/j.cell.2010.03.006. PubMed: 20303867.

15. Ho MK, Su Y, Yeung WW, Wong YH (2009) Regulation of transcription factors by heterotrimeric G proteins. Curr Mol Pharmacol 2: 19-31. doi: 10.2174/1874-470210902010019. PubMed: 20021442.

16. Hu X, Chen J, Wang L, Ivashkiv LB (2007) Crosstalk among Jak-STAT, Toll-like receptor, and ITAM-dependent pathways in macrophage activation. J Leukoc Biol 82: 237-243. doi:10.1189/jlb.1206763. PubMed: 17502339.

17. O'Sullivan LA, Liongue C, Lewis RS, Stephenson SE, Ward AC (2007) Cytokine receptor signaling through the Jak-Stat-Socs pathway in disease. Mol Immunol 44: 2497-2506. doi:10.1016/j.molimm. 2006.11.025. PubMed: 17208301.

18. Chang L, Karin M (2001) Mammalian MAP kinase signalling cascades. Nature 410: 37-40. doi:10.1038/35065000. PubMed: 11242034.

19. Pimkova K, Bockova M, Hegnerova K, Suttnar J, Cermak J et al. (2011) Surface plasmon resonance biosensor for the detection of VEGFR-1-a protein marker of myelodysplastic syndromes. Anal Bioanal Chem.

20. Zubair A, Burbelo PD, Vincent LG, Iadarola MJ, Smith PD et al. (2011) Microfluidic LIPS for serum antibody detection: demonstration of a rapid test for HSV-2 infection. Biomed Microdevices 13: 1053-1062. doi: 10.1007/s10544-011-9575-x. PubMed: 21826483.

21. Geng T, Bao N, Litt MD, Glaros TG, Li L et al. (2011) Histone modification analysis by chromatin immunoprecipitation from a low number of cells on a microfluidic platform. Lab Chip 11: 2842-2848. doi: 10.1039/c1lc20253g. PubMed: 21750827.

22. Chen X, Kapil MA, Hughes AJ, Herr AE (2011) Single-microchannel, multistep assay reports protein size and immunoaffinity. Anal Chem 83: 6573-6579. doi:10.1021/ac200982j. PubMed: 21834519.

23. Ciaccio MF, Wagner JP, Chuu CP, Lauffenburger DA, Jones RB (2010) Systems analysis of EGF receptor signaling dynamics with microwestern arrays. Nat Methods 7: 148-155. doi:10.1038/nmeth. 1418. PubMed: 20101245.

CHAPTER 4

DOT BLOTTING USING MICROFLUIDIC TECHNIQUES

Abstract

Cell cytokine detection has important applications in biological sciences and clinical medicine due to cytokine's roles in cellular communication, immune response, and inflammation. There is an increasing demand for high-throughput cytokine detection technology, but current approaches can be costly and therefore have limited accessibility. To overcome some of these limitations, we have designed a microfluidic dot blotting system that is cost-effective and increases the throughput. Dot blots of cell supernatants were spotted onto a poly(vinylidene fluoride) (PVDF) membrane and sandwiched between a glass slide and a microfluidic device. Antibodies were introduced into the microfluidic channels and multiple different antibodies were run in the channels simultaneously. To achieve high-throughput by maximizing the number of channels on a dot, we studied the device channel spacing design constraints impacted by surface hydrophobicity and protein concentrations. Also, we described the use of the microfluidic system for profiling lipopolysaccharide (LPS)-stimulated cytokine secretion in macrophages.

4.1 Introduction

Cytokines are vital biomolecules that transmit signals when they are released from one cell and are sensed by another cell. The information carried by cytokine proteins can play significant roles in cellular communication, immune response, and inflammation. To detect cytokines in body fluids, immunoassays are the most common adopted techniques. Immunoassays can detect cytokines at low concentrations. There are different types of immunoassays that can be applied for cytokine detection such as ELISA [1], flow cytometry [2], antibody array assays [3], and bead-based assays [4]. Although the traditional approaches are effective in cytokine detection, they can be costly and technically challenging; thus have limited applications for point-of-care medical device development.

Considering cytokine production is associated with a large number of diseases and measurement of cytokines is important in disease diagnosis [5-7], there is a growing demand for a reliable and cost-effective cytokine detecting assay that can collect large amount of cytokine information within limited amount of samples. Recently, developments in bead-based assays, multilayer membrane dot blotting system, and electroluminescence assays have been applied as multiplex assays to detect multiple cytokines in small amount of samples [8-10]. However, these approaches can be far from being cost-effective and being a simple system with potential in point-of-care diagnosis development. Furthermore, these advanced approaches and the most standard cytokine detection method of ELISA usually require special instruments for signal readout.

To overcome the limitations of the aforementioned immunoassays for cytokine detection, we have developed a microfluidic dot blot system with the ability of profiling multiple cytokines simultaneously. The system was assembled by interfacing a microfluidic polydimethylsiloxane (PDMS) device to a polyvinylidene fluoride (PVDF) membrane so that microfluidic channels are placed on protein dots. The good sealing at the PDMS-PVDF interface provided a miniaturized flow chamber for antibody-antigen binding interaction and therefore protein probing. Moreover, to improve the detection efficiency as a multiplex assay, it is critical that a large number of channels can be placed within a given size of protein dot. The number of channels allowed within a certain size of dot is primarily determined by channel spacing and can be impacted by several variables. We studied two variables that are most relevant to experimental conditions: surface wetting property and protein sample concentration. Using the microfluidic system on a PVDF platform, we demonstrated a convenient, simple, and reagent-saving inflammatory cytokine detection assay with detection efficiency 4-folds higher and antibody-consumption 2000-fold less.

4.2 Materials and Methods

Microfluidic device design

The microfluidic device was designed using SolidWork (CAD/Art Services, Inc.; Bandon, OR USA) to generate a CAD file. Each lane contains 5 channels. Each channel has the dimensions of length 1.985 cm, width 150 μm, channel spacing 0.107 cm, and depth 150 μm. In our device design we have 5 lanes (25 channels in total).

PDMS Microfluidic Device fabrication

The transparency mask was printed using a CAD file of the microfluidic device (CAD/Art Services, Inc.; Bandon, OR USA). Soft-lithography was used to fabricate a silicon master mold from the transparency mask. The microfluidic devices were created by mixing the pre-polymer and curing agent at a 12:1 weight ratio (Sylgard 184 Silicone Elastomer Kit, Dow Corning; Midland, MI USA) and then pouring the mixture onto a silicon master mold that had been affixed to a smooth aluminum tray. The amount of silicone used in this process was titrated such that the devices produced were 6 mm thick. To remove the bubbles from the silicone mixture, the tray was placed in a degassing apparatus until all bubbles were gone (~15 minutes). The aluminum tray was then transferred into an oven that was pre-heated to 100°C where it was baked for 90 minutes. The aluminum tray was removed from the oven and allowed to cool at room temperature until it could be handled comfortably (~45 minutes). To remove the microfluidic device from the aluminum pan, a razor blade was used to cut around the silicon master mold. The microfluidic device was then slowly peeled away from the silicon master mold. The excess silicone was trimmed from the device using the razor blade such there was a ~1 cm perimeter around the channels; this perimeter insures a good seal between the microfluidic device and the glass slide that is used during the injection process.

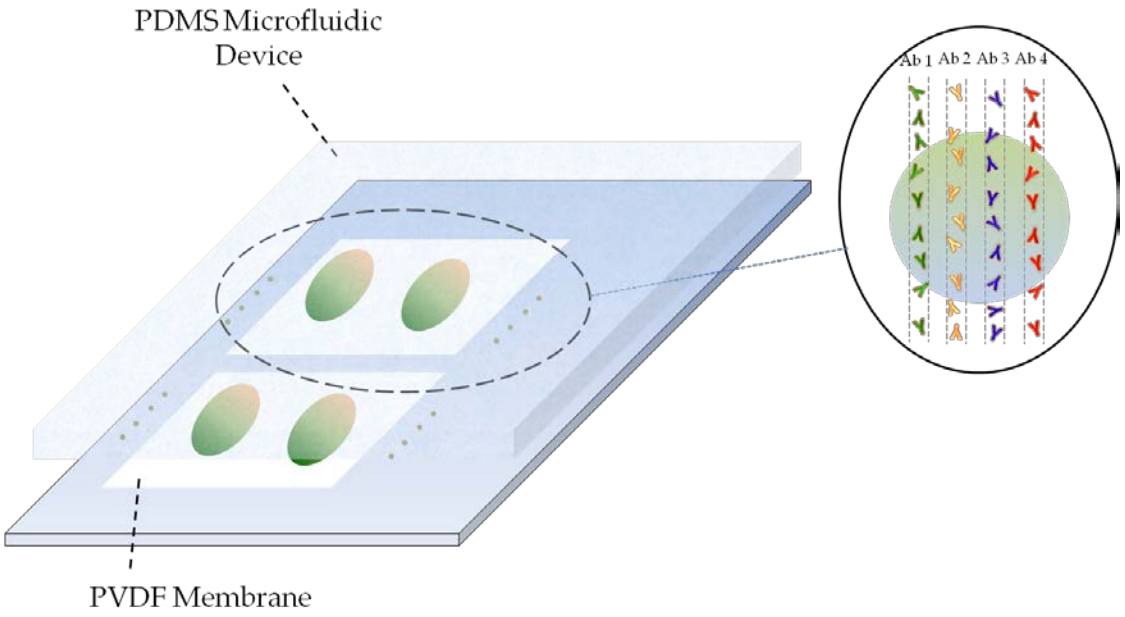

Figure 4.1. Schematic of microfluidic dot blot system.

Proteins are deposited as circular dots on PVDF membrane. The microfluidic PDMS device is assembled by incorporating the device to the membrane. The microfluidic channels are placed on protein sample dots. Antibodies are introduced in each microfluidic channel.

Preparation of Protein Samples

The BSA (bovine serum albumin) protein samples were prepared by dissolving BSA (Fisher BioReagents™ Bovine Serum Albumin, Fraction V, Heat Shock Treated) in deionized water at concentrations of 0.25 mg/ml, 0.025 mg/ml, 0.0125mg/ml, and 0.0025 mg/ml.

The bone-marrow derived macrophages (BMDMs) were collected from mouse C57/BL6 received from Charles River. The bone-marrow cells were strained in 100um filter, spilt into 12 petri dishes with 10-L929-cell conditioned media. BMDMs plated in 6-well plates at 10^6/ml then put on MCSF. Cells were washed in PBS-Ca/-mg and incubated in 0.5% FBS medium containing lipopolysaccharide (LPS) from *Escherichia coli* O55:B5 (Sigma-Aldridge; St Louis, MO USA) at a concentration of 100 ng/ml. Cell supernatants were collected at 48 hour time point. The supernatant samples were spun down at 2500xg for 4 minutes at 4°C. Then transferred the supernatant to new tubes and store them at -80°C for preservation.

Preparation of PVDF Membrane Immobilized with BSA using microfluidics

Prior to protein immobilization, the PVDF membrane was ‘wetted’ by immersing it in methanol for 10 seconds, DI water for 2 minutes and finally TBS for 5 minutes. The PVDF membrane was then placed on top of stack of dry filter papers and covered with a single piece of filter paper that had been soaked in TBS buffer. The membrane hydrophobicity was changed by varying the time (15 min, 30 min, 45 min, and 1 hour) spent between placing the membrane on the filter paper stack, and immobilizing protein on the membrane surfaces. In studies where the impact of protein concentration was evaluated, membranes were allowed to dry for 3 minutes to yield a contact angle of 55°.

To immobilize BSA protein on PVDF membrane using a microfluidic device, the PVDF membrane was removed from the filter paper stack, laid on a glass slide, subsequently the PDMS microfluidic device was placed on the top. Solutions of BSA at concentrations of 0.25 mg/ml, 0.025 mg/ml, 0.0125mg/ml, and 0.0025 mg/ml were injected at different channels using a 1ml syringe with 27G ½ needles and incubated for 15 minutes. Following the protein solution incubation, the microfluidic device channels was washed with TBS buffer by injection then the

PDMS device was removed and the membrane was dried at the room temperature for at least 3 hours.

Contact angle measurement for PVDF membrane hydrophobicity evaluation

Static water contact angle measurements were performed using a CAM 100 Optical Contact Meter (KSV Instruments). Water contact angles were measured on PVDF membrane dried at the time points of 15 min, 30 min, 45 min, and 1 hour. The contact angles were evaluated by fitting a mathematical expression to the shape of the drop and then calculating the slope of the tangent to the drop at the liquid-solid interface line at the left and the right side of the droplet (for further analysis average values were used).

Quantification and statistical analysis of protein lane width

To visualize the protein lane on the PVDF membrane, the membrane was incubated in a solution of 7% acetic acid, 10% methanol and incubated for 15 minutes. Once incubation is completed, the membrane was washed in DI water for 5 minutes for four times. The membrane was stained with SYPRO ruby red (Life Technologies; Carlsbad, CA USA) for 15 minutes then washed with DI water for 1 min for four times.

Protein blots were scanned using Gel Doc XR system (BioRad). The images were imported into ImageJ software and analyzed. The microfluidic protein blots with the signal intensity in the channel region was measured. The signal intensity and position profile was plotted at upstream, middle-stream, and downstream. The position profile was fit by Gauss model and full width half maximum (FWHM) was extracted. Quantification is expressed as means with standard deviations (SD) with numbers of individual experiments repeated for three times.

Microfluidic dot blot for cytokine detection

For cytokine detection using dot blot, PVDF membrane was wet with methanol for 10 seconds, rinsed in DI water for 2 minutes then in TBS buffer for 5 minutes. The PVDF membrane was placed on a stack of filter paper with dry filter paper at the bottom and filter paper wetted with TBS buffer on the top. Then 8-10 µL of cell supernatant per dot were spotted onto wet PVDF membrane. Once the cell supernatants wicked into the PVDF membrane, the membrane was removed from the filter paper and placed on a clean surface to dry overnight.

Once dry, the microfluidic device was placed on the PVDF membrane with channels aligned on the dots. IL6, IFNγ, amd IL10 primary antibodies were injected into each channel and incubated for 30 minutes. Both the primary and secondary antibody dilutions were prepared in 0.1% BSA and 0.1% Tween20 TBS. Following the primary antibody incubation period, the channels were washed with TBS buffer injection then the microfluidic device was removed and the membrane was blocked for 30 minutes in 0.1% BSA and 0.1% Tween20 TBS. The membrane was then incubated with the secondary antibody for 1 hour prior to chemiluminescent detection with alkaline phosphatase.

4.3 Results and Discussion

Sealing condition test at the interface of microfluidic PDMS device and PVDF membrane

Our first goal was to test the sealing at PDMS and PVDF interface and compare the test characteristics of conventional dot blot with microfluidic dot blot. In our previous work, we have demonstrated the feasibility of using microfluidic PDMS device on PVDF membrane at antibody incubation step for Western blot [11]. However, in dot blot protein samples are directly deposited on PVDF membrane without the electroblotting step. To test if leakage would be an issue in applying microfluidics to dot blot, we collected cell supernatants from both LPS treated macrophages and no treatment group and spotted the supernatants on PVDF membrane as dots. Using primary antibody IL6, an inflammatory cytokine, at three different concentrations (1:100; 1:500; 1:1000), we compared the signals between the conventional approach and microfluidic dot blot. The microfluidic dot blot approach resulted in slightly lower, but comparable signal intensities compared to those from traditional dot blotting. In both approaches, the signals and signal variation were comparable under the conditions tested.

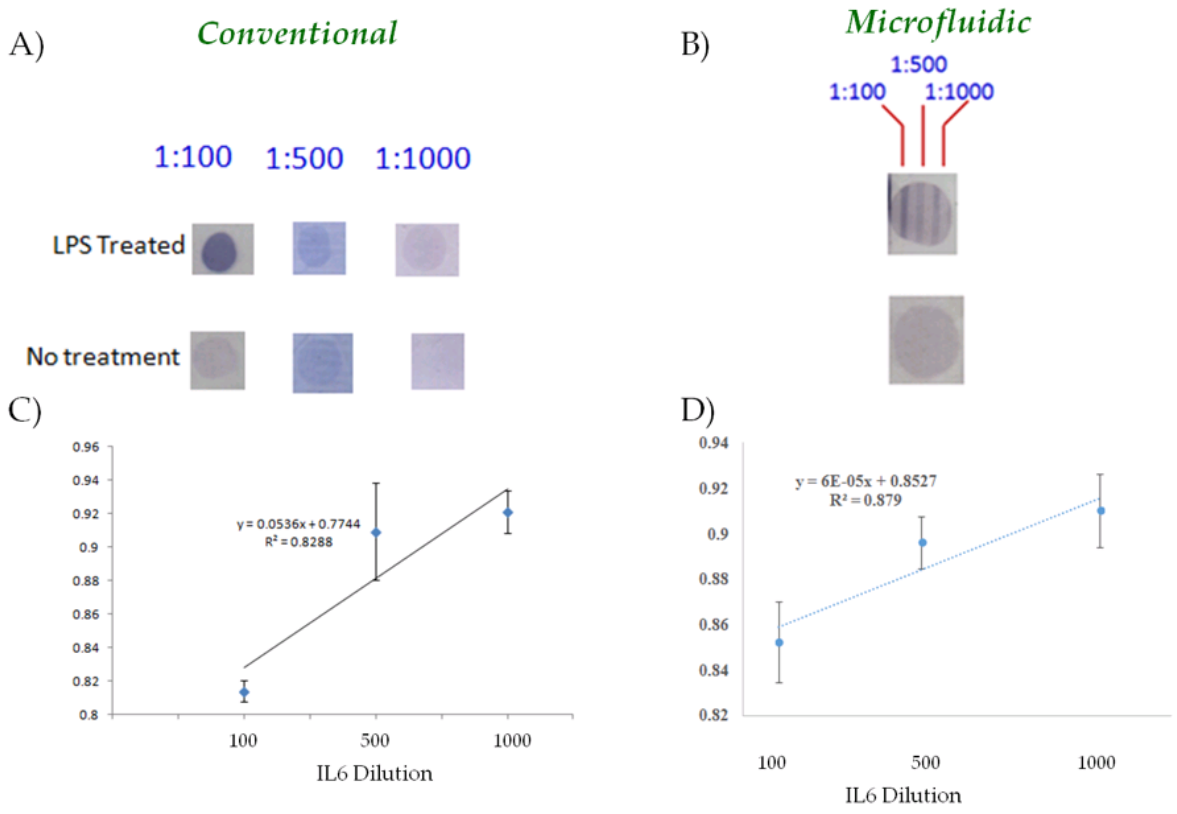

Figure 4.2. Comparison of traditional and microfluidic dot blotting in macrophage supernatants.

Representative dot blots for IL6 at three antibody dilutions (1:100; 1:500; 1:1000) using (A) conventional and (B) microfluidic dot blotting techniques. The signal intensity for the (C) conventional and (D) microfluidic blots were quantified using ImageJ software and normalized to the background signal. Immunoblots are representative of three independent PVDF membranes from the same macrophage supernatants.

Influence of protein concentration on protein lane width using a microfluidic device on PVDF

We next determined the microfluidic device channel spacing design constraints by measuring protein lane width variation. Since antibody flow on PVDF membrane is governed by adsorption and diffusion, antibody solution at different concentrations might result in different lane width [12]. We developed an approach by studying the lane width of immobilizing model protein BSA at different concentrations on PVDF membrane. The model protein BSA was chosen at a concentration range that is tested in most biology studies, 2.5 mg/ml, 25 µg/ml, 12.5 µg/ml, and 2.5 µg/ml. The dimension of the PDMS microfluidic device is 3.1 cm long, 150 µm wide, and

100 μm deep. Protein lane width measurement was conducted by first placing the PVDF membrane on a glass slide with the microfluidic device on the top. Model protein BSA solutions were injected into the channels and incubated for 15 minutes. The microfluidic device was then removed and the PVDF membrane was dried for at least 2 hours. To detect the protein lane signal, the entire PVDF membrane was incubated with Sypro Ruby protein blot stain fluorescent dye. The detection was achieved by scanning the membrane with Gel DOC EZ system. The image was analyzed in ImageJ by measuring the line profile of signal intensity at three positions: upstream, middle stream, and downstream. The peak intensity was fitted by Gauss model at each position using Origin software to get the full-width-half-maximum (FWHM).

The dependence of protein width on the protein sample concentration is shown in Figure 3. The signal intensity decreases as protein concentration decreases. This implies protein concentration should be taken into consideration for device design constraints in our microfluidic PDMS on PVDF membrane system. The measurement of actual protein lane width on PVDF membrane at highest concentration of 2.5 mg/ml is approximately 200 μm (Appendix). The measurement provides guidelines of channel spacing design with consideration of the widest protein lane width.

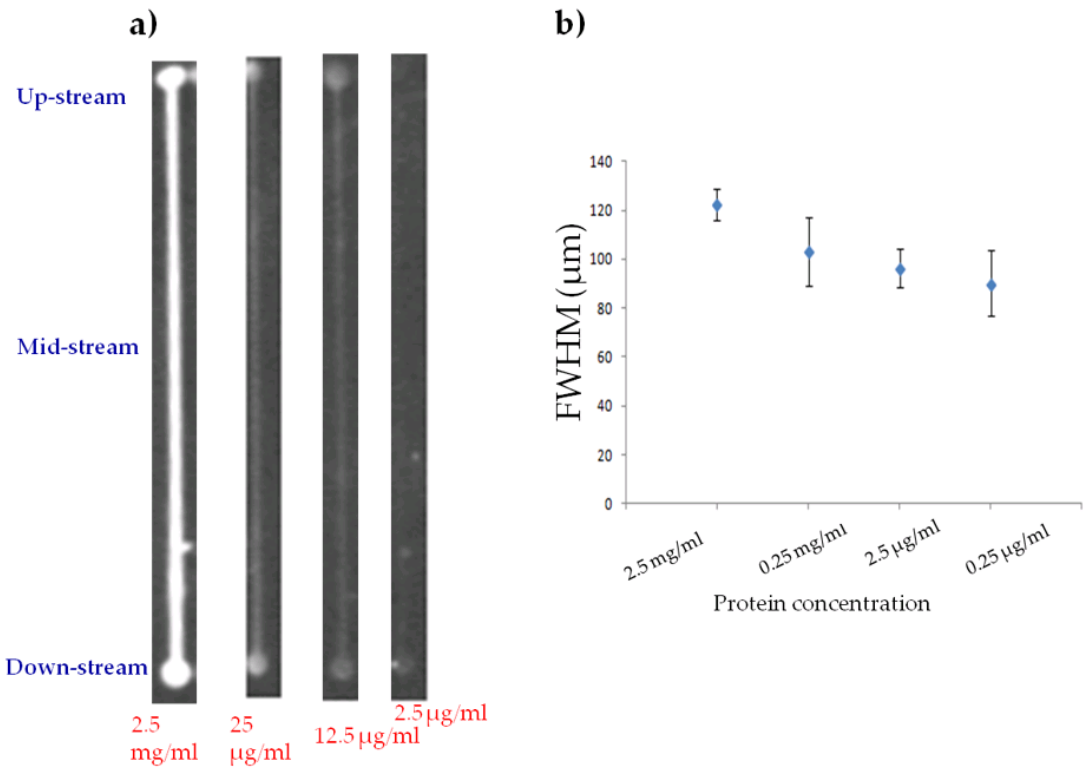

Figure 4.3. Protein lane width variation at different protein concentrations.

(A) Ruby red stain of BSA protein at different concentrations immobilized on PVDF membrane using a microfluidic device. (B) Full-width-half-maximum (FWHM) measurement of channel width at three different positions, up-stream, mid-stream, and down-stream. The FWHM values were taken by fitting the intensity profile with Guass model. The values of FWHM at three different positions were averaged at each protein concentration and show a decreasing trend as protein concentrations get low. This suggests protein concentration within the range tested should be taken into consideration for microfluidic device channel spacing design. Results are representative of three independent experiments.

Influence of PVDF hydrophobicity on protein lane width using a microfluidic device

The surface wetting property is another variable that influences liquid spreading area on a surface. Surface hydrophobicity or hydrophilicity can be quantitatively defined by contact angle. Hydrophobic surface has large contact angle whereas hydrophilic surface has small contact angle [13-15]. PVDF membrane is a good platform to control its surface wetting property. PVDF membrane becomes hydrophilic when it is activated with methanol then washed with DI water. The hydrophilic membrane can then be placed on a dry, clean filter paper and water evaporation changes the membrane surface to become hydrophobic. To study the influence of surface wetting property on protein lane width, we first activated PVDF membrane with methanol and rinsed in

DI water, then the membrane was placed in the air (on clean filter paper) and dried at different time points (15 min, 30 min, 45 in, 60 min). The surface wetting property of PVDF membrane drying at different time points was quantified by contact angle measurement. Once the PVDF membrane got dried at the testing condition, the membrane was then removed from the filter paper and assembled between a glass slide and a microfluidic device. BSA protein solution at the concentration of 25 μg/ml was injected into the microfluidic channel and incubated for 15 minutes. After the incubation, the procedures of Ruby red stain and signal detection by Gel DOC EZ system as described above were followed. The same data analysis of using ImageJ for line profile measurement and Gauss peak fitting in Origin software was adopted.

Figure 4 shows the protein lane width variation at different surface wetting properties. The mean and standard variations of FWHM measured at different surface wetting properties suggest that there is no significant difference between any groups of the time points we chose to study. These results further suggest that channel spacing in the microfluidic device design is not impacted by the surface hydrophobicity conditions that were tested.

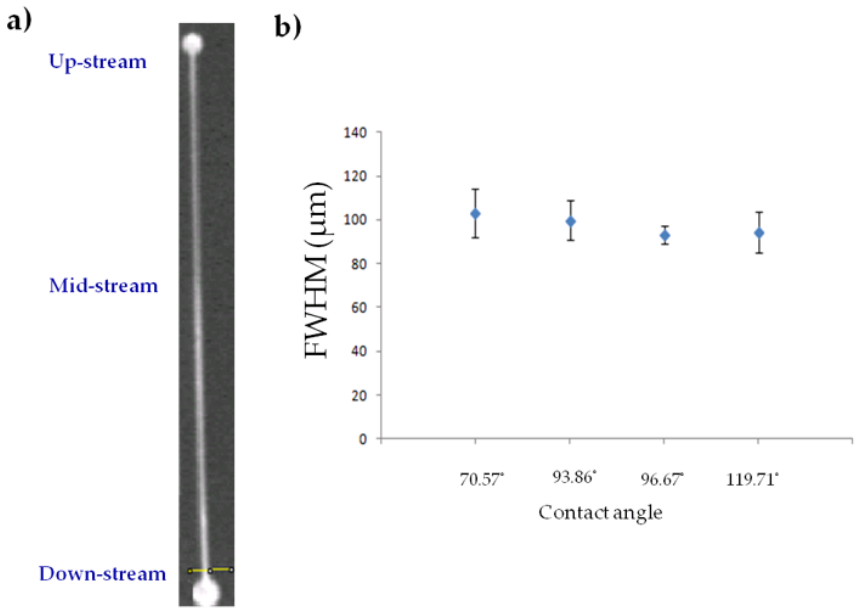

Figure 4.4. Protein lane width variation at different PVDF membrane surface wetting properties.

(A) Representative image of Ruby red stain of BSA protein immobilized on PVDF membrane at different surface wetting properties using a microfluidic device. (B) Full-width-half-maximum

(FWHM) measurement of BSA protein lane width with PVDF membrane at different contact angles. The FWHM values were taken at three different positions, up-stream, mid-stream, and down-stream by fitting the intensity profiles with Guass model. The values of FWHM at three different positions were averaged at each contact angle and do not show a significant difference among different groups. This suggests substrate hydrophobicity within the range tested should not change microfluidic device channel spacing design. Results are representative of three independent experiments.

Monitoring multicomponent, inflammatory cytokines

Immune systems are often modulated by cytokine released in human bodies. Monitoring these secreted proteins by the immune cells plays an important role in manipulating inflammatory responses and diseases. Like macrophages, the dominant phagocytes of the immune system, they release a variety of different inflammatory cytokines once they are activated [16-18].

These complexities limit the ability of using the standard and best validated method Enzyme-Linked Immuno-Sorbant Assay (ELISA) in inflammatory molecule studies with high efficiency, low-cost, and wide accessibility [8]. We believe that some of these challenges could be addressed using microfluidic dot blotting system. To determine the efficacy of the microfluidic dot blotting system for cytokine detection, we stimulated RAW264.7 cells with LPS (100 ng/ml) for 48 hours and collected cell lysates. We probed for interleukin 6 (IL-6), interleukin 10 (IL-10), interferon gamma (IFNγ), and netrin-1 with traditional and microfluidic dot blotting (Figure 4). Traditional dot blotting required preparation of four protein blots. In contrast, microfluidic dot blotting obtained similar results using only one set of protein blot. By simultaneously probing cytokines released in macrophage supernatants, we demonstrated the feasibility of minimizing the time and resources compared using a simple approach.

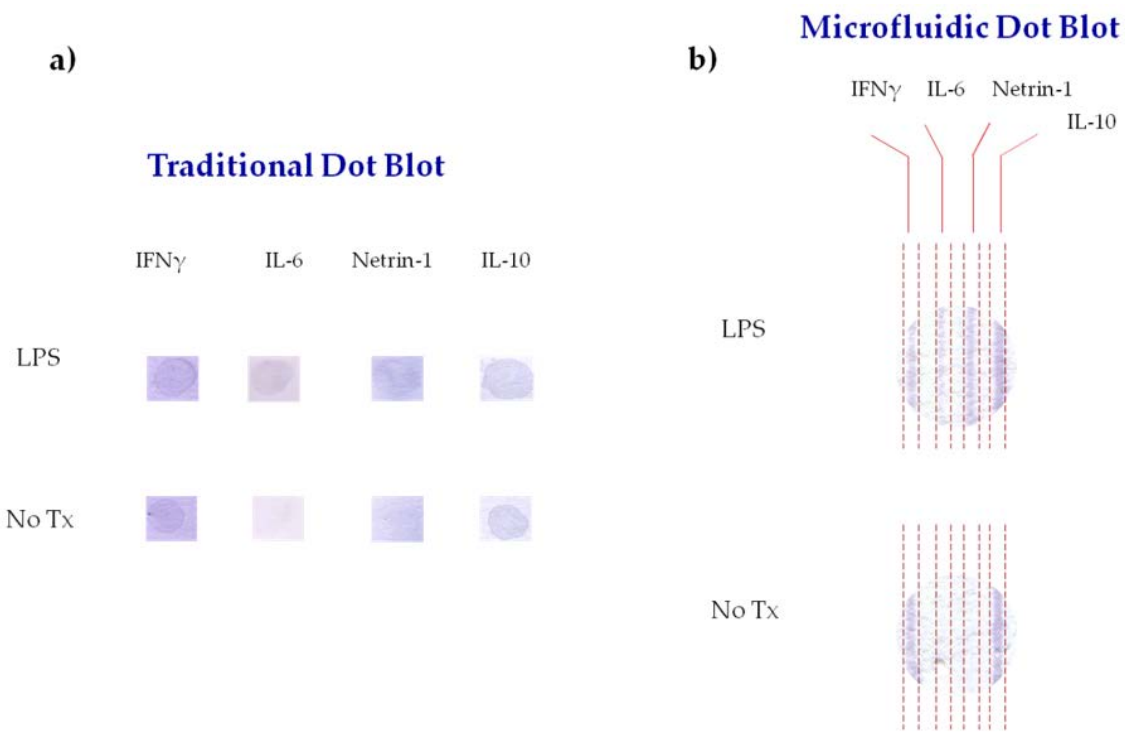

Figure 4.5. Detection of inflammatory cytokines in response to inflammatory stimuli.

(A) Traditional dot blots of macrophage supernatants probing for IFNγ, IL-6, Netrin-1, and IL-10 in response to LPS stimulation. The signal intensities of IL-6 and netrin-1 changed in LPS-treated and no treatment groups. (B) Microfluidic dot blots on same macrophage supernatants as (A). The signal intensity change from microfluidic dot blots demonstrates comparable and reproducible test results. The microfluidic device allows for simultaneous monitoring of four different cytokines in the same sample. Results are representative of three independent experiments.

4.4 Discussion

In this study, we designed a cost-effective microfluidic dot blot device that can be used to probe for inflammatory cytokines efficiently. We further investigated device design constraints under some certain conditions. Microfluidic dot blot is a technically simple and resource-saving approach that can be easily applied in common biological labs and clinical settings. The microfluidic dot blot approach simplifies sample preparation process by directly depositing protein samples on a PVDF membrane. We designed the device with channel width to be 150 μm and chose alkaline phosphatase chemiluminescent substrate as a labeling technique. This provides the advantages of seeing distinguishable bands as signals with the naked eye, so that additional tools or instruments are not required.

In summary, microfluidic dot blot allows the detection of multiple proteins in one sample simultaneously with only microliters of antibody needed. This method provides an excellent approach for cytokine analysis with applications in biological research and disease diagnosis.

Appendix

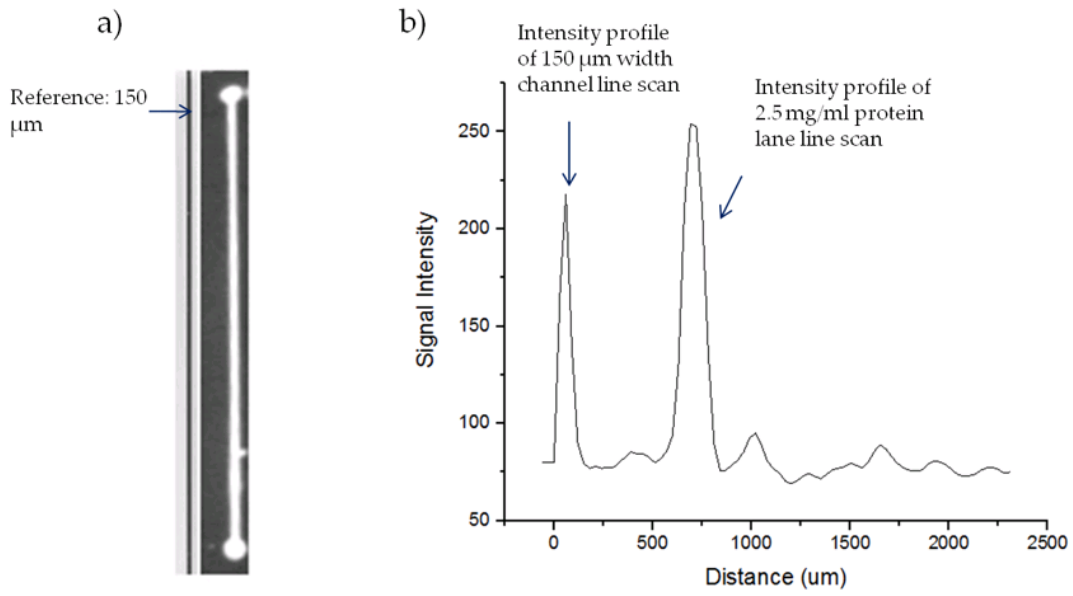

Figure 4.6. 2.5 mg/ml protein lane width measurement by intensity profile line scan.

(A) 2.5 mg/ml protein lane width image was scanned together with the transparency mask of a microfluidic channel. The channel width is 150 µm. (B) Intensity profile by line scan of 150 µm wide channel and 2.5 mg/ml protein lane. The base width of 2.5 mg/ml protein lane is approximately 200 µm compared to the 150 µm lane.

4.5 References

1. Evanoff, H.L., et al., *A sensitive ELISA for the detection of human monocyte chemoattractant protein-1 (MCP-1).* Immunol Invest, 1992. **21**(1): p. 39-45.
2. Jung, T., et al., *Detection of intracellular cytokines by flow cytometry.* J Immunol Methods, 1993. **159**(1-2): p. 197-207.
3. Sakai, A., et al., *Profiling the cytokines in gingival crevicular fluid using a cytokine antibody array.* J Periodontol, 2006. **77**(5): p. 856-64.
4. Elshal, M.F. and J.P. McCoy, *Multiplex bead array assays: performance evaluation and comparison of sensitivity to ELISA.* Methods, 2006. **38**(4): p. 317-23.
5. Boyle, M.D., et al., *Application of immunoproteomics to rapid cytokine detection.* Methods, 2006. **38**(4): p. 342-50.
6. Eckmann, L., *Innate immunity and mucosal bacterial interactions in the intestine.* Curr Opin Gastroenterol, 2004. **20**(2): p. 82-8.
7. Patel, G.P., D.P. Gurka, and R.A. Balk, *New treatment strategies for severe sepsis and septic shock.* Curr Opin Crit Care, 2003. **9**(5): p. 390-6.
8. Leng, S.X., et al., *ELISA and multiplex technologies for cytokine measurement in inflammation and aging research.* J Gerontol A Biol Sci Med Sci, 2008. **63**(8): p. 879-84.
9. Galperin, M.M., et al., *Multimembrane dot-blotting: a cost-effective tool for proteome analysis.* Biotechniques, 2004. **36**(6): p. 1046-51.
10. Elshal, M.F. and J.P. McCoy, *Multiplex bead array assays: Performance evaluation and comparison of sensitivity to ELISA.* Methods, 2006. **38**(4): p. 317-323.
11. Chang, H.N., et al., *Profiling inflammatory responses with microfluidic immunoblotting.* PLoS One, 2013. **8**(11): p. e81889.
12. Hansen, C.L., et al., *A robust and scalable microfluidic metering method that allows protein crystal growth by free interface diffusion.* Proc Natl Acad Sci U S A, 2002. **99**(26): p. 16531-6.
13. Gao, L. and T.J. McCarthy, *A perfectly hydrophobic surface (thetaA/thetaR = 180 degrees /180 degrees).* J Am Chem Soc, 2006. **128**(28): p. 9052-3.
14. Quere, D., *Non-sticking drops.* Reports on Progress in Physics, 2005. **68**(11): p. 2495-2532.

15. Good, R.J., *Contact-Angle, Wetting, and Adhesion - a Critical-Review.* Journal of Adhesion Science and Technology, 1992. **6**(12): p. 1269-1302.
16. Scull, C.M., W.D. Hays, and T.H. Fischer, *Macrophage pro-inflammatory cytokine secretion is enhanced following interaction with autologous platelets.* J Inflamm (Lond), 2010. **7**: p. 53.
17. Murray, R.Z. and J.L. Stow, *Cytokine Secretion in Macrophages: SNAREs, Rabs, and Membrane Trafficking.* Front Immunol, 2014. **5**: p. 538.
18. O'Shea, J.J. and P.J. Murray, *Cytokine signaling modules in inflammatory responses.* Immunity, 2008. **28**(4): p. 477-87.

CHAPTER 5
CONCLUSIONS

5.1 Summary

As the life expectancy of human beings is rising, the proportion of healthcare costs is expected to rise. The costs will be highly likely to be used to provide better healthcare services including effective treatment and efficient disease diagnosis. Disease diagnosis and the decision-making for treatments rely on reliable, low cost, and efficient immunoassays. In this dissertation, the immunoassay development goals was addressed by first exploring the potential of using graphene as an immunoassay sensing platform with detailed characterization (Chapter 2). Then the work of applying microfluidic techniques to immunoblot with the advantages of reducing the cost and improving the efficiency is presented (Chapter 3). Based on this achievement, the microfluidic technique was applied again to dot blot and device design constraints impacted by surface hydrophobicity and protein concentration were tested (Chapter 4). These studies contribute to the immunoassay development goals of sensitivity, cost reduction, efficiency, and point-of-care diagnosis development. These studies are believed to be valuable for development of graphene biosensing platform and application of microfluidic technique to protein blotting. In this chapter, the roles of the works of graphene biosensing platform development and applying microfluidic techniques to immunoblot and dot blot were discussed individually in the greater scheme of scientific research. Then the general lessons and principles that have learned through the development of these techniques and possible future directions are presented.

5.2 Summary of functionalization of graphene

In 2004, the initial success of isolating single atomic layer graphene by Geim and Novoselov generated ripples of excitement in the scientific community. Since then, a tremendous number of potential applications of graphene have been proposed ranging from supercapacitors to DNA-sequencing, photocatalysts, and display. This opens new avenues for research of understanding the properties of graphene and urges the development of a variety of functionalization methods

for the following reasons: (1) graphene is inert, which weakens its competitive strength in many fields of application, and (2) graphene possesses zero band gap and therefore has limited application potential in nanoelectronic devices.

Several chemical approaches of graphene functionalization have been developed to make graphene broadly applicable. In general, for covalent functionalization of graphene, there are two routes: (1) forming covalent bonds between carbon atoms (C=C) and free radicals or dienophiles, and (2) attaching organic functional groups to the oxygen groups of graphene oxide (GO) then reduce GO by removing the oxygen groups and rehybridize the sp^3 C atoms to sp^2 C atoms. GO has been extensively studied as the starting material to covalently link organic groups to the surface. However, nowadays the methods to completely reduce GO to graphene is still under investigation. It remains to be a study of interest to completely remove all residual epoxy or hydroxyl functional groups left on reduced graphene oxide.

5.2.1 Functionalization of graphene: covalent approaches

Considering the fact that the complete reduction of GO to graphene has not yet been achieved, forming a reaction between graphene carbon atoms and free radicals or dienophiles is currently the most attractive approach. Moreover, this approach has also been shown to be an effective functionalization method with other carbon nanomaterials. For example, this approach of adding dienophiles to C=C bonds has been successfully applied in the functionalization of carbon nanostructures including fullerenes, nanotubes, and nanoribbons. This type of reaction is flexible and important because it offers the ability to react with a variety of functional groups. Moreover, the results have displayed interesting applications in many fields ranging from polymer composites, to biotechnology, nanoelectronic devices, drug delivery, and solar cells [1].

With the motivation of understanding more about the fundamental properties of the functionalized graphene, the information about features such as functional group density and uniformity would be of great interest. The functional group density is often quantitatively estimated by calculating the I_D/I_G ratio in Raman spectroscopy. This ratio indicates the ratio between carbon atoms with sp^2 and sp^3 hybridization in the graphene lattice. This can be used as an estimation of the degree of covalent functionalization reaction but does not reveal actual coupling efficiency nor the uniformity.

This dissertation addresses the goals of estimating the coupling species density and their uniformity on functionalized graphene surface using an approach of conjugating fluorophore to the functionalized graphene. This approach introduces new elements on the functionalized graphene sheets and therefore provides the feasibility of estimating the functional group coupling efficiency by the XPS spectra. Moreover, conjugating fluorophore to graphene surface provides the feasibility of visualizing the graphene sheet under fluorescence microscopy. The fluorophores conjugated to graphene sheet emit fluorescence instead of being completely quenched. Moreover, the uniform fluorescence on the graphene sheet indicates the functional groups are created uniformly on the surface. The approach introduced in this dissertation provides a novel method that fulfills both requirements of estimating the functional group density and characterizing the uniformity.

5.3 Advantages of using graphene as an immunoassay platform

The material graphene is a promising candidate material to be studied as an alternative to common immunoassay platform materials. Common types of existing immunoassay platform materials include polystyrene in 96-well plate in ELISA, glass substrate in surface-plasmon resonance (SPR) detection, and nanoparticles in pathogen or proteins detection [2, 3]. Polystyrene and glass, however, are bulky and stiff materials, that can crack under stress and collision. Nanoparticles might get aggregated in solution and change the physical and chemical properties such as transport property and reactivity. These material properties limit the use of immunoassays as *in vitro* assays used only in a lab-based or hospital-testing environment.

In contrast, graphene is an atom-layer thin carbon material with high mechanical strength (approximately 60 times stronger than glass and 3000 times stronger than polystyrene), low weight (approximately 1 million times lighter than the same size glass sheet), and high flexibility. The thin size, high mechanical strength, low weight, and flexibility of graphene open opportunities to build immunoassays on flexible and portable platforms. Because graphene is also biocompatible and non-toxic in the human body, this advancement could result in point-of-care disease screening and diagnosis, and on-site and timely monitoring immunoassays. One promising application would be to use graphene immunoassays for real-time biological response monitoring *in vivo*. For example, it has been shown that a functionalized graphene sheet can be transferred onto the surface of a tooth for pathogenic bacteria monitoring of tooth enamel. This

demonstrates the potential of using graphene for *in vivo*, *in situ*, and real-time biomolecule detection development [4].

The sensitivity of immunoassays can also be improved from using graphene. Graphene is an ideal 2-dimensional material with high surface-to-volume ratio. Its geometric structure as a planar sheet, the sp^2 hybridized form of carbon atoms, and the development of different approaches to attach biomolecules on functionalized graphene surface all lead to high antibody immobilization density on graphene surface. This results in high detection sensitivity and low limit of detection with the sensitivity of up to 80 times higher if graphene-based immunoassays are compared to the commercial ELISA [5]. Moreover, graphene exhibits several special electrical/physical material properties that make it an immunoassay platform suitable for versatile detection mechanism development. Graphene has high electrical conductivity (3000 W/m-K), high surface-to-volume-ratio (2600 m^2/g), and a high electron transfer rate, all of which contribute to high sensitivity in graphene-based electrochemical immunoassays [6]. Finally, the optical properties of graphene have also been widely explored in immunoassay platform development.. Graphene is transparent over a broad wavelength spectrum from ultraviolet to infrared, and graphene can quench fluorescence efficiently. Graphene's quenching mechanism has been applied in fluoroimmunoassay applications with a goal of building high selectivity assays that are suitable in antibody-antigen binding or releasing events detection [7]. Altogether these material properties of graphene suggest that it will be highly suitable as a versatile and competitive alternative material in immunoassay platform development.

5.4 Future steps of developing graphene biosensing platform

For the biosensing application, carbon nanotubes (CNT) and graphene are the most promising carbon nanomaterials with great potential in development. However, there are still needs to be addressed to meet future requirements. One of the areas which is essential and deserves expanded attention in graphene biosensing development is keeping protein biomolecules in the active state on graphene surface. In protein immobilization on solid substrates, there is often a trade-off between firmly immobilizing capture proteins, binding sufficient protein amount, and maintaining protein structure and function in the assay format [8].

In this dissertation, a method has been developed to covalently immobilize proteins on a large scale graphene surface. Covalent bonds are strong and can withstand the washing steps in many

immunoassay procedures, but covalent linkage can also denature some proteins. Furthermore, graphene is intrinsically hydrophobic. This raises the concern that strong interaction of proteins with the graphene surface through hydrophobic interaction may lead to unexpected protein folding that could disturb protein stability and activity. Therefore, one direction of interest for future study is to determine antibodies immunoreactivity when they are immobilized on graphene surface [9, 10].

In summary, protein immobilization onto a solid surface has great significance in numerous applications including protein analysis, drug screening, and medical diagnostics. As graphene has raised great interests as a material candidate for biosensing platform, the work presented here advances the field by developing an approach to provide the information about the density and the uniformity of proteins immobilized on a large size graphene sheet surface.

5.5 Summary of applying microfluidic techniques to immunoblotting

In the second part of this thesis, the incorporation of microfluidic techniques to protein immunoblotting was developed with the purpose of reducing antibody consumption and cost. A microfluidic device was designed and fabricated and can be easily interfaced with the existing protein immunoblotting systems. In contrast to traditional blotting that incubates the whole membrane in antibody solution, a microfluidic device was used so that the antibody solution is only needed in the microfluidic channels. It has been shown that immunoblotting with microfluidic technique can perform quantitative analysis with comparable results to the traditional protein immunoblotting. The PVDF-based immunoblotting system is useful with an assortment of antibodies, both monoclonal and polyclonal, and works in a wide range of primary and secondary antibody concentrations. It has also been demonstrated that the designed microfluidic systems can be used with a variety of antibodies to profile signaling pathways and can achieve comparable detection limits. Compared to the current existing techniques for protein expression profiling such as fluorescent bead assays (Luminex), enzyme-linked immunosorbent assays (ELISAs), and protein microarrays, the microfluidic approach developed in this thesis is less expensive, requires no special instruments or tools, provides a simple technique for detecting multiple proteins, and offers wider accessibility for clinical diagnostics and research groups.

Our system was built by placing a microfluidic PDMS device on a protein PVDF membrane. The results show that the sealing condition of a PDMS device to a PVDF membrane is good and requires no additional surface treatments to prevent leaking. This is promising in incorporating PVDF membrane-based immunoassay with microfluidics considering membrane based microfluidic techniques often suffers the leakage issues with clamping fixation [11]. Our results show that hydrophobic PVDF membranes can be easily incorporated into microfluidic devices without additional complicated surface modification such as plasma treatment. Moreover, PVDF membranes' protein binding capacity can be easily increased by adding Tween-20, a type of surfactant, to the antibody solution. The additive Tween-20 generates pores on the PVDF membrane and therefore provides adequate binding capacity for proteins [12]. The concentration of Tween-20 was optimized so that the membrane gets activated by simply flowing antibody solution with Tween-20 in the microfluidic channel.

Considering the advantages of simple integration of a PVDF membrane to a microfluidic system, PVDF membranes' high protein binding capacity (150 – 160 μg/cm^2) and high mechanical strength, PVDF membranes' wide application in many immunoassay set up, and the practicality of eye visualization for signal detection, the developed techniques are believed to have the potential to be easily prototyped and be used in most biology labs and clinical settings [13].

5.6 Summary of cytokine detection using microfluidic dot blotting

In the third project, microfluidic technique was applied to dot blotting and the device design constraints of channel spacing impacted by PVDF membrane surface hydrophobicity and protein sample concentrations were further investigated. Microfluidic assisted dot blotting technique brings in the advantages of reducing antibody consumption and probing multiple proteins simultaneously. Both dot blotting and immunoblotting (Chapter 3) are techniques used for protein probing. However, in dot blotting protein samples are directly deposited on PVDF membrane whereas in immunoblotting proteins are transferred by electroblotting. It has been shown that the sealing condition is good at the interface of a microfluidic device and a PVDF membrane with electroblotting (Chapter 3) and without electroblotting (Chapter 4).

In microfluidic dot blotting system, the capability of probing multiple proteins was determined by the number of channels placed on a certain size of antigen dot. Large number of channels can

be obtained if the channel spacing is small. However, this also results in higher risks of cross-contamination when different antibodies flow adjacent. The influence of common experimental conditions on channel spacing was studied using an approach of immobilizing BSA protein on a PVDF membrane with a microfluidic device. The impacts of protein concentrations and surface wetting properties on BSA lane width were tested. Within the range tested, the results suggest that protein lane width shows distinguishable variation when protein concentrations are changed. The width does not show much difference when surface wetting properties are changed. The microfluidic dot blotting system has been shown to be capable for relevant biological tests by detecting the inflammation cytokines secreted by macrophages. The microfluidic dot blotting system provides a simple and cost-effective approach to develop multiplex cytokine assays with great potential in biological research and point-of-care device development.

5.7 Future steps for applying microfluidic techniques to immunoblotting and dot blotting

The developed microfluidic techniques can simultaneously capture multiple proteins from a single sample, therefore the expression and activity of several signaling mediators in response to numerous treatments can be quantitatively measured in a single experiment. This implied the microfluidic technique is a potentially powerful tool for multiplex protein immunoassays, which is of particular interest because there is a growing need to simultaneously screen multiple proteins in a single sample [14]. However, to simultaneously detect multiple proteins in different concentration ranges, high sensitivity and good signal-to-noise ratio are critical. The following address the issues that deserve further consideration.

5.7.1 Surface Modification and Immobilization

Nonspecific adsorption or binding to molecules rather than analytes is a key concern in immunoassays. The adsorption of non-targeted biomolecules often degrades the sensitivity and specificity, and also lowers the signal to noise ratio. Protein molecules can adsorb to PVDF membranes non-specifically because of the membrane's structure. PVDF membrane is a network of pockets and channels of different dimensions, this heterogeneity provides the ability for proteins to adsorb non-specifically due to hydrogen bonding, charge interactions, or non-polar interactions [15].

Currently non-specific binding is still a challenging issue in immunoassay development and is

often solved by blocking. Blocking agents such as bovine serum albumin, casein and detergents are commonly used in many immunoassays, but they rarely reduce protein non-specific binding completely. Another approach is to use surface functionalization or modification on the substrate surface. For example, to reduce non-specific protein binding interaction on hydrogel, an effective approach was to use Poly(ethylene) Glycol (PEG) to modify the surface. PEG can also be grafted on PVDF membrane, so the proposed future direction is to study the non-specific binding on microfluidic protein immunoblot using PVDF membrane with PEG modification [16, 17].

5.8 Prospects

Nowadays, immunoassays are essential to the practice of health care worldwide and are still considering of a growing demand due to the expanding use in point-of-care diagnostics, cancer diagnosis, tissue typing, infectious disease screening, hormone detection, and therapeutic drug monitoring. Moreover, the advance in nanotechnology leads to immunoassays' improvements in efficiency, sensitivity, specificity, and cost reduction. Various techniques have been applied to immunoassay development including quantum dots [18], microcantilever [19], bead-based assays, and microfluidics. However, these laboratory-based, high-end technologies are not so much applicable in resources-limited settings and poor countries. Responding to these initiatives, recently there is an emerging trend of applying cheap and simple technologies to immunoassay development especially for disease diagnosis [20].

One of the essential immunoassay components is the platform. Our graphene functionalization and characterization work suggests a potential of using CVD graphene as a biosensing platform. As large scale and low cost CVD graphene are available nowadays, this is promising in exploiting graphene as a cheap immunoassay platform. However, there are still many questions need to be addressed and conditions such as sensitivity and limit of detection need to be tested.

In the second and the third parts of the dissertation, microfluidic systems for immunoblots and dot blots were developed. The developed approaches are validation of multiplex protein assays and they can be used to detect biological samples in small volumes. With the flexibility in antibodies, labeling substrates (horseradish peroxidase or alkaline phosphatase), and simple integration, it is anticipated that the microfluidic systems can be widely applied to reduce the cost for protein analysis in most biology labs and in clinical settings.

5.9 References

1. Georgakilas, V., et al., *Functionalization of Graphene: Covalent and Non-Covalent Approaches, Derivatives and Applications.* Chemical Reviews, 2012. **112**(11): p. 6156-6214.
2. Ranzoni, A., et al., *One-step homogeneous magnetic nanoparticle immunoassay for biomarker detection directly in blood plasma.* ACS Nano, 2012. **6**(4): p. 3134-41.
3. Lin, F.Y., et al., *Development of a nanoparticle-labeled microfluidic immunoassay for detection of pathogenic microorganisms.* Clin Diagn Lab Immunol, 2005. **12**(3): p. 418-25.
4. Eckert, M.A. and W.A. Zhao, *Opening windows on new biology and disease mechanisms: development of real-time in vivo sensors Introduction.* Interface Focus, 2013. **3**(3).
5. Vashist, S.K., *Graphene-based immunoassay for human lipocalin-2.* Anal Biochem, 2014. **446**: p. 96-101.
6. Tang, J., et al., *Magneto-Controlled Graphene Immunosensing Platform for Simultaneous Multiplexed Electrochemical Immunoassay Using Distinguishable Signal Tags.* Analytical Chemistry, 2011. **83**(13): p. 5407-5414.
7. Demchenko, A.P. and M.O. Dekaliuk, *Novel fluorescent carbonic nanomaterials for sensing and imaging.* Methods and Applications in Fluorescence, 2013. **1**(4).
8. Fici, D.A., et al., *A protein multiplex microarray substrate with high sensitivity and specificity.* Journal of Immunological Methods, 2010. **363**(1): p. 60-66.
9. Holtz, B., et al., *Denaturing and refolding of protein molecules on surfaces.* Proteomics, 2007. **7**(11): p. 1771-1774.
10. Camarero, J.A., *Recent developments in the site-specific immobilization of proteins onto solid supports.* Biopolymers, 2008. **90**(3): p. 450-458.
11. Kim, D. and A.E. Herr, *Protein immobilization techniques for microfluidic assays.* Biomicrofluidics, 2013. **7**(4).
12. Chang, H.H., et al., *The effect of Tween-20 additive on the morphology and performance of PVDF membranes.* Journal of Membrane Science, 2014. **466**: p. 302-312.
13. Ivanov, S.S., et al., *Antibodies immobilized as arrays to profile protein post-translational modifications in mammalian cells.* Molecular & Cellular Proteomics, 2004. **3**(8): p. 788-795.

14. Han, K.N., C.A. Li, and G.H. Seong, *Microfluidic Chips for Immunoassays.* Annual Review of Analytical Chemistry, Vol 6, 2013. **6**: p. 119-141.
15. Li, Q.A., Z.L. Xu, and M. Liu, *Preparation and characterization of PVDF microporous membrane with highly hydrophobic surface.* Polymers for Advanced Technologies, 2011. **22**(5): p. 520-531.
16. Charles, P.T., et al., *Reduction of Non-Specific Protein Adsorption Using Poly(ethylene) Glycol (PEG) Modified Polyacrylate Hydrogels In Immunoassays for Staphylococcal Enterotoxin B Detection.* Sensors, 2009. **9**(1): p. 645-655.
17. Chang, Y., et al., *Surface grafting control of PEGylated poly(vinylidene fluoride) antifouling membrane via surface-initiated radical graft copolymerization.* Journal of Membrane Science, 2009. **345**(1-2): p. 160-169.
18. Chan, W.C.W., et al., *Luminescent quantum dots for multiplexed biological detection and imaging.* Current Opinion in Biotechnology, 2002. **13**(1): p. 40-46.
19. Lee, J.H., et al., *Immunoassay of prostate-specific antigen (PSA) using resonant frequency shift of piezoelectric nanomechanical microcantilever.* Biosensors & Bioelectronics, 2005. **20**(10): p. 2157-2162.
20. Yetisen, A.K., M.S. Akram, and C.R. Lowe, *Paper-based microfluidic point-of-care diagnostic devices.* Lab on a Chip, 2013. **13**(12): p. 2210-2251.